NACA

RESEARCH MEMORANDUM

AERODYNAMIC STUDY OF A WING-FUSELAGE COMBINATION
EMPLOYING A WING SWEPT BACK 63° - EFFECT OF
REYNOLDS NUMBER AT SUPERSONIC MACH
NUMBERS ON THE LONGITUDINAL CHARAC-
TERISTICS OF A WING TWISTED AND
CAMBERED FOR UNIFORM LOAD

By John C. Heitmeyer

Ames Aeronautical Laboratory
Moffett Field, Calif.

NATIONAL ADVISORY COMMITTEE
FOR AERONAUTICS
WASHINGTON
October 9, 1950

~~CONFIDENTIAL~~

NATIONAL ADVISORY COMMITTEE FOR AERONAUTICS

RESEARCH MEMORANDUM

AERODYNAMIC STUDY OF A WING—FUSELAGE COMBINATION EMPLOYING A WING
SWEPT BACK 63° — EFFECT OF REYNOLDS NUMBER AT SUPERSONIC
MACH NUMBERS ON THE LONGITUDINAL CHARACTERISTICS
OF A WING TWISTED AND CAMBERED
FOR UNIFORM LOAD

By John C. Heitmeyer

SUMMARY

Results of a wind—tunnel investigation of the longitudinal charac-
teristics of a wing—body combination employing a wing with leading edge
swept back 63° are presented. The model wing, which was cambered and
twisted to support a uniform load at a lift coefficient of 0.25 at a
Mach number of 1.53, had an aspect ratio of 3.5 and a taper ratio of
0.25. Lift, drag, and pitching—moment measurements were made in the
Reynolds number range from 0.75 million to 3.7 million at Mach numbers
between 1.2 and 1.53. The experimentally determined lift—curve slope
and aerodynamic—center position for the wing—fuselage model are compared
with theoretical values for the wing alone modified to include the
effects of the elastic deformation of the wing.

The data indicated that at the lower test Mach numbers, at which
the trailing edge of the wing is subsonic, and in the range of Reynolds
numbers between 0.75 million and about 2.0 million viscous effects
influenced the lift—curve slope, position of the aerodynamic center, and
minimum drag coefficient to a significant degree. The data further
indicated, however, that between Reynolds numbers of about 2.0 million
and 3.7 million little change in the parameters occurred.

INTRODUCTION

In reference 1, it was pointed out that theoretical lift—drag ratios
of 10 or greater could be obtained at moderate supersonic speeds by
sweeping the wings back within the Mach cone from the apex of the
leading edge. To obtain experimental data for this type of model con-
figuration, a general investigation of the aerodynamic characteristics
of a wing—body combination employing a wing with leading edge swept back
63° was undertaken at the Ames Aeronautical Laboratory.

~~CONFIDENTIAL~~

The present investigation and that of reference 2 were undertaken to obtain experimental data on the longitudinal characteristics of a large—scale model. Whereas reference 2 considers the effects of Mach number, the present report will consider the effects of Reynolds number on the longitudinal characteristics of the twisted and cambered, 63° swept—back, wing—fuselage model.

NOTATION

a.c.	aerodynamic center measured at zero lift, percent of the mean aerodynamic chord
b	wing span measured perpendicular to plane of symmetry, feet
c	projection of local wing chord in the wing reference plane[1] and measured parallel to plane of symmetry, feet
$\bar{c}$	mean aerodynamic chord $\left(\dfrac{\int_0^{b/2} c^2\,dy}{\int_0^{b/2} c\,dy}\right)$, feet
C_D	drag coefficient
$C_{D_{min}}$	minimum drag coefficient
C_L	lift coefficient
C_{L_α}	slope of the lift curve measured at zero lift, per degree
C_m	pitching—moment coefficient referred to mean aerodynamic chord and measured about quarter—chord point of the mean aerodynamic chord
L/D	lift—drag ratio
$(L/D)_{max}$	maximum lift—drag ratio
M	Mach number
q	dynamic pressure, pounds per square foot
R	Reynolds number, based on mean aerodynamic chord
S	projected wing area in the wing reference plane including area in the region formed by extending leading and trailing edges to plane of symmetry, square feet

---

[1]Wing reference plane is defined as the plane containing the swept leading edge of the wing. For the model of the present investigation, the wing reference plane contains the root chord, that is, the wing chord in the plane of symmetry.

---

y   distance measured perpendicular to plane of symmetry in the wing reference plane, feet

α   angle of attack of the wing reference plane, degrees

THEORETICAL CONSIDERATIONS

The theoretical calculations of lift–curve slope and position of the aerodynamic center were made for the wing alone and were based on the linearized theory of compressible flow. Within the order of accuracy of the linear theory, the lift–curve slope and position of the aerodynamic center are independent of camber and twist and depend only upon the wing plan form. The methods of references 3 and 4 were used, therefore, to compute the values of lift–curve slope and position of the aerodynamic center.

Reference 5 has shown that, for highly swept wings as used in the present investigation, the effects of elastic deformation may be sizable and must be considered when calculating the lift–curve slope and the position of the aerodynamic center. The bending deflection is a function of the lift of the wing which is related directly to the angle of attack of the root section and to the dynamic pressure. In the present investigation, the magnitude of the effect of elastic deformation upon the lift–curve slope and the position of the aerodynamic center varied throughout the Reynolds number range, since changes in the Reynolds number were accomplished by changing the dynamic pressure of the tunnel air stream.

The theoretical values of lift–curve slope and position of the aerodynamic center were modified to account for the effects of the elastic deformation of the wing at the different dynamic pressures. An experimentally measured twist due to elastic deformation was utilized with the equations and methods of reference 5 to calculate the ratios for the elastic to rigid wing of the lift–curve slope and the position of the aerodynamic center. To determine the twist due to elasticity the angle of attack of the tip section was measured throughout the angle–of–attack range of the wing–fuselage model at each of the test Reynolds numbers. The difference between the measured tip section angles of attack and the geometric twist (3.52° washout) per unit angle of attack of the model is presented in figure 1. The sense of the twist due to elastic deformation is to increase the wing washout at angles of attack above the angle of zero lift.

The theoretical values of the lift–curve slope and of the position of the aerodynamic center do not include the effects of the fuselage or wing–fuselage interference.

EXPERIMENTAL CONSIDERATIONS

Apparatus

Wind tunnel.— The present investigation was conducted in the Ames 6— by 6—foot supersonic wind tunnel. A complete description of the wind tunnel and of its flow characteristics is given in reference 6.

Model.— The model of reference 2 was used in the present investigation and is shown mounted in the test section of the tunnel in figure 2. The dimensions of the model are presented in figure 3. The wing plan form had the leading edge swept back 63°, a taper ratio of 0.25, and an aspect ratio of 3.5. Sections parallel to the plane of symmetry were composed of NACA 64A005 thickness distributions and a=1.0—type mean lines, the maximum camber of which were determined by the method of reference 1. The variation of maximum camber with spanwise station is presented in figure 4. The theoretical spanwise twist as determined by reference 1 was modified to account for the twist due to deflection of the wing under the design load for a dynamic pressure of 1100 pounds per square foot. (The dynamic pressure corresponding to a Mach number of 1.53 at a tunnel total pressure of 18 pounds per square inch absolute.) The theoretical twist was further modified to reduce the large twist at the root indicated by theory. The variation of twist of the model with spanwise station is shown in figure 4. The angle of twist was measured with respect to the wing reference plane. The incidence, that is, the angle between the root chord and the fuselage center line measured in the plane of symmetry, was zero.

The wing and the fuselage were constructed of steel. The entire model was painted and sanded to a smooth finish.

Instrumentation.— The four—component, strain—gage balance and methods of instrumentation of this investigation were identical to that described in reference 2.

Test Methods

Range of test variables.— Lift, drag, and pitching—moment measurements, along with base—pressure readings, were made at Reynolds numbers between 0.75 million and 3.7 million, and at test Mach numbers between 1.2 and 1.53. The angle of attack was varied from 0° to 10° in approximately 1—1/4° increments. The dynamic pressure varied from 150 pounds per square foot at the lowest Reynolds number to 800 pounds per square foot at the highest Reynolds number.

Reduction of data.— All force and moment coefficients are based upon the total projected wing area, including the area in the region formed by extending the leading and trailing edges to the plane of symmetry. The pitching-moment coefficient is based upon the mean aerodynamic chord and referred to the quarter point of that chord. The Reynolds number is also based upon the mean aerodynamic chord.

The wing reference plane was used as the reference for angle-of-attack measurements. Normal and chord forces as measured by the strain-gage balance were resolved into lift and drag forces.

Corrections to data.— Reference 6 indicates that the air stream in the wind-tunnel test section has significant axial and vertical pressure gradients, but that in the horizontal cross-stream direction the pressure gradient is negligible. When the model was mounted with the wings vertical, the principal effect of the stream irregularities was to produce a force in the longitudinal direction as it has been shown that small yaw angles caused by the vertical pressure gradient had negligible effect upon the longitudinal characteristics. The force in the longitudinal direction was obtained by integrating the product of the static pressure and the change in cross-sectional area of the body along the body length. It was shown in reference 6 that the static-pressure-coefficient variation along the tunnel center line was independent of tunnel total pressure, and consequently the coefficient form of the drag correction was the same at all Reynolds numbers.

For the ratio of sting diameter to base diameter used, reference 7 indicates that the effect of sting interference is confined to a change in base pressure. By the same reasoning used in reference 2, the drag of the model was corrected by an amount equal to the product of the base area and the difference between the measured base pressure and the free-stream static pressure at that point.

Precision of data.— The manner in which the final uncertainty in any quantity was obtained is the same as that described in reference 2, since the experimental techniques were identical.

The following table lists the final uncertainty in the quantities at zero angle of attack and at the highest and lowest Reynolds number of the investigation:

Quantity	0.75 million	3.7 million
Lift coefficient	±0.0025	±0.0005
Drag coefficient	.0005	.0002
Pitching-moment coefficient	.0009	.0002
Angle of attack	.04°	.04°
Reynolds number	.03 million	.03 million
Mach number	.01	.01

RESULTS AND DISCUSSION

General Characteristics

The lift coefficient as a function of angle of attack is presented in figure 5 for the range of Reynolds numbers and Mach numbers investigated. The data indicate linear variation of lift coefficient with angle of attack to a lift coefficient of about 0.2. Above this value the rate of change of lift coefficient with angle of attack decreased.

Pitching-moment coefficient as a function of lift coefficient is presented in figure 6. The slope of the pitching-moment curve, a measure of the static longitudinal stability, was constant to a lift coefficient of about 0.2. Above a lift coefficient of 0.2 the slope of the pitching-moment curve was less negative, indicating decreased static stability. Above a lift coefficient of approximately 0.4 further increase in lift coefficient resulted in an unstable variation of pitching moment with lift.

The loss in lift and the decrease in static stability at the larger lift coefficients $(C_L > 0.2)$ are associated with the spanwise flow of the upper-surface separated turbulent boundary layer on the outboard sections of the wing near the trailing edge. Tuft pictures taken during the investigation showed spanwise flow of the boundary layer to be present in this region at lift coefficients above 0.2 at all test Mach numbers and Reynolds numbers.

Drag coefficient and lift-drag ratio as functions of lift coefficient are presented in figures 7 and 8, respectively. The data of figure 8 indicated that, within the range investigated, Reynolds number had little effect upon the lift-drag ratio.

Effect of Reynolds Number

The experimental and the theoretical values of the lift-curve slope and of the position of the aerodynamic center as functions of Reynolds number are presented in figures 9 and 10, respectively. As noted previously, the theoretical curves are those for the wing alone and for the wing considered as an elastic beam. The theoretical values of lift-curve slope and position of the aerodynamic center for the rigid wing alone are indicated on the margins of figures 9 and 10, respectively.

With a change in Reynolds number, the lift-curve slope and the position of the aerodynamic center were subjected to the combined influence of elastic deformation of the model and to viscosity effects. The effect of elastic deformation is shown by the difference between the theoretical

values of the elastic wing and the corresponding value of the rigid wing.
The difference between the theoretical curve of the elastic wing and the
experimental wing—fuselage data is due in part to the limitations of the
linear theory, to wing—body interference, to the presence of the fuse—
lage, and to viscosity effects. The effects of viscosity upon the lift—
curve slope and upon the position of the aerodynamic center are indicated,
however, by the variation with Reynolds number of the difference between
the experimental curve and the respective theoretical curve of the elastic
wing.

Lift—curve slope.— The rate of change of the difference between the
experimental and the theoretical curve of the elastic wing indicates that
the lift—curve slope, at the lower Mach numbers, was most influenced by
viscosity effects in the range of Reynolds numbers between 0.75 million
and about 2.0 million. The variation of lift—curve slope, measured at
zero lift, in this range is believed to be related to separation of the
laminar boundary layer in the steep adverse pressure gradient in the
region of the subsonic trailing edge. Reference 8 has shown that at low
Reynolds numbers it is possible for the lifting pressures, in the region
behind the trailing—edge Mach line, to be greater than the corresponding
lifting pressures at higher Reynolds numbers. With an increase in
Reynolds number, the area of separated laminar boundary layer was reduced
by the onset of turbulent flow with a subsequent reduction in lift—curve
slope.

In the Reynolds number range from about 2.0 million to 3.7 million,
however, the difference between the experimental and theoretical curve
was nearly constant, indicating little change in the lift—curve slope due
to viscosity effects. The apparent decrease in lift—curve slope with
Reynolds number in this range, shown in figure 9, is associated with the
elastic deformation of the wing mentioned previously.

Aerodynamic center.— The aerodynamic center at zero lift as a
function of Reynolds number is presented in figure 10. The variation
with Reynolds number of the difference between the theoretical and experi—
mental curves shown in figure 10 indicates that viscosity effects caused
a forward movement of the experimental aerodynamic center between
Reynolds numbers of 0.75 million and about 2.0 million. As noted pre—
viously, the influence of the subsonic trailing edge resulted in higher
lifting pressures in the region behind the trailing—edge Mach line at
the lowest Reynolds numbers (reference 8). The lifting pressures in this
region decreased as the Reynolds number was increased, resulting in the
forward movement of the aerodynamic center. At a Reynolds number of
about 2.0 million, the boundary layer in this region had apparently
become fully turbulent and no perceptible movement of the experimental
aerodynamic center occurred with increased Reynolds number up to the
maximum test value of 3.7 million.

Pitching—moment coefficient at zero lift.— The experimental results
(fig. 6) show that, at all the test Mach numbers, the pitching—moment

coefficient at zero lift decreased in the range of Reynolds numbers between 0.75 million and about 2.0 million, and remained essentially unchanged in the range of Reynolds numbers between about 2.0 million and 3.7 million. It is believed that the behavior at the lower Reynolds numbers is related to the large areas of separated laminar flow, present at such small Reynolds numbers, reducing the effective camber of the wing sections. Increasing the Reynolds number from 0.75 million to about 2.0 million reduced the amount of separation, thereby increasing the effective camber of the wing sections, with the consequent decrease in the pitching-moment coefficient at zero lift.

Minimum drag coefficient.— The minimum drag coefficient is plotted as a function of Reynolds number in figure 11. The decrease in minimum drag coefficient as the Reynolds number was increased from 0.75 million to about 2.0 million is believed to be related to a decrease in pressure drag due to a reduction in the area of separated laminar flow. This reasoning is substantiated by the liquid—film studies of reference 9 which showed that the area of separated flow decreased between Reynolds numbers of 0.34 million and 0.68 million. This favorable effect should continue until transition from laminar to turbulent boundary layer has occurred on the wing surface. As noted previously, the boundary layer on the wing surface behind the trailing—edge Mach line was apparently fully turbulent above a Reynolds number of about 2.0 million. The slight increase in minimum drag coefficient which occurred above a Reynolds number of about 3.0 million appeared to be due to either turbulent sep-aration near the trailing edge or an increase in skin—friction drag due to the longer run of turbulent boundary layer brought about by the transition point moving forward of the trailing—edge Mach line. (See reference 10.) The variation of minimum drag with Reynolds number was, in general, independent of Mach number.

Maximum lift—drag ratio.— The variation of maximum lift—drag ratio with Reynolds number is shown in figure 12. As the Mach number was decreased, the variation of maximum lift—drag ratio with Reynolds number became greater. This is believed to be attributable to the greater effects of viscosity at the lower Mach numbers associated with the steep chordwise pressure gradients which appear when the Mach line from the wing trailing edge extends well forward over the wing surface.

CONCLUSIONS

The results of the investigation of the effects of Reynolds number on the longitudinal characteristics of a wing—body configuration employ-ing a wing with leading edge swept back 63° indicated:

1. At each of the test Mach numbers and from about 2.0 million to 3.7 million Reynolds number, little change in values of the test param-eters occurred.

2. The values of the lift-curve slope and minimum drag coefficient decreased and the position of the aerodynamic center moved forward as the Reynolds number increased from 0.75 million to about 2.0 million.

3. The variation of lift-curve slope, aerodynamic-center position, and minimum drag coefficient in the range of Reynolds numbers between 0.75 million and about 2.0 million can be attributed to the greater effects of viscosity which manifest themselves in the region behind the trailing-edge Mach line.

Ames Aeronautical Laboratory,
     National Advisory Committee for Aeronautics,
          Moffett Field, Calif.

REFERENCES

1. Jones, Robert T.: Estimated Lift-Drag Ratios at Supersonic Speed. NACA TN 1350, 1947.

2. Hall, Charles F., and Heitmeyer, John C.: Aerodynamic Study of a Wing-Fuselage Combination Employing a Wing Swept Back 63°. — Characteristics at Supersonic Speeds of a Model With the Wing Twisted and Cambered for Uniform Load. NACA RM A9J24, 1950.

3. Cohen, Doris: The Theoretical Lift of Flat Swept-Back Wings at Supersonic Speeds. NACA TN 1555, 1948.

4. Cohen, Doris: Theoretical Loading at Supersonic Speeds of Flat Swept-Back Wings with Interacting Trailing and Leading Edges. NACA TN 1991, 1949.

5. Frick, C. W., and Chubb, R. S.: The Longitudinal Stability of Elastic Swept Wings at Supersonic Speed. NACA TN 1811, 1949.

6. Frick, Charles W., and Olson, Robert N.: Flow Studies in the Asymmetric Adjustable Nozzle of the Ames 6- by 6-Foot Supersonic Wind Tunnel. NACA RM A9E24, 1949.

7. Perkins, Edward W.: Experimental Investigation of the Effects of Support Interference on the Drag of Bodies of Revolution at a Mach Number of 1.5. NACA RM A8B05, 1948.

8. Boyd, John W., Katzen, Elliott D., and Frick, Charles W.: Investigation at Supersonic Speed (M=1.53) of the Pressure Distribution Over a 63° Swept Airfoil of Biconvex Section at Several Angles of Attack. NACA RM A8F22, 1948.

9. Madden, Robert T.: Aerodynamic Study of a Wing-Fuselage Combination Employing a Wing Swept Back 63°.— Characteristics at a Mach Number of 1.53 Including Effect of Small Variations of Sweep. NACA RM A8J04, 1949.

10. Frick, Charles W., and Boyd, John W.: Investigation at Supersonic Speed (M=1.53) of the Pressure Distribution over a 63° Swept Airfoil of Biconvex Section at Zero Lift. NACA RM A8C22, 1948.
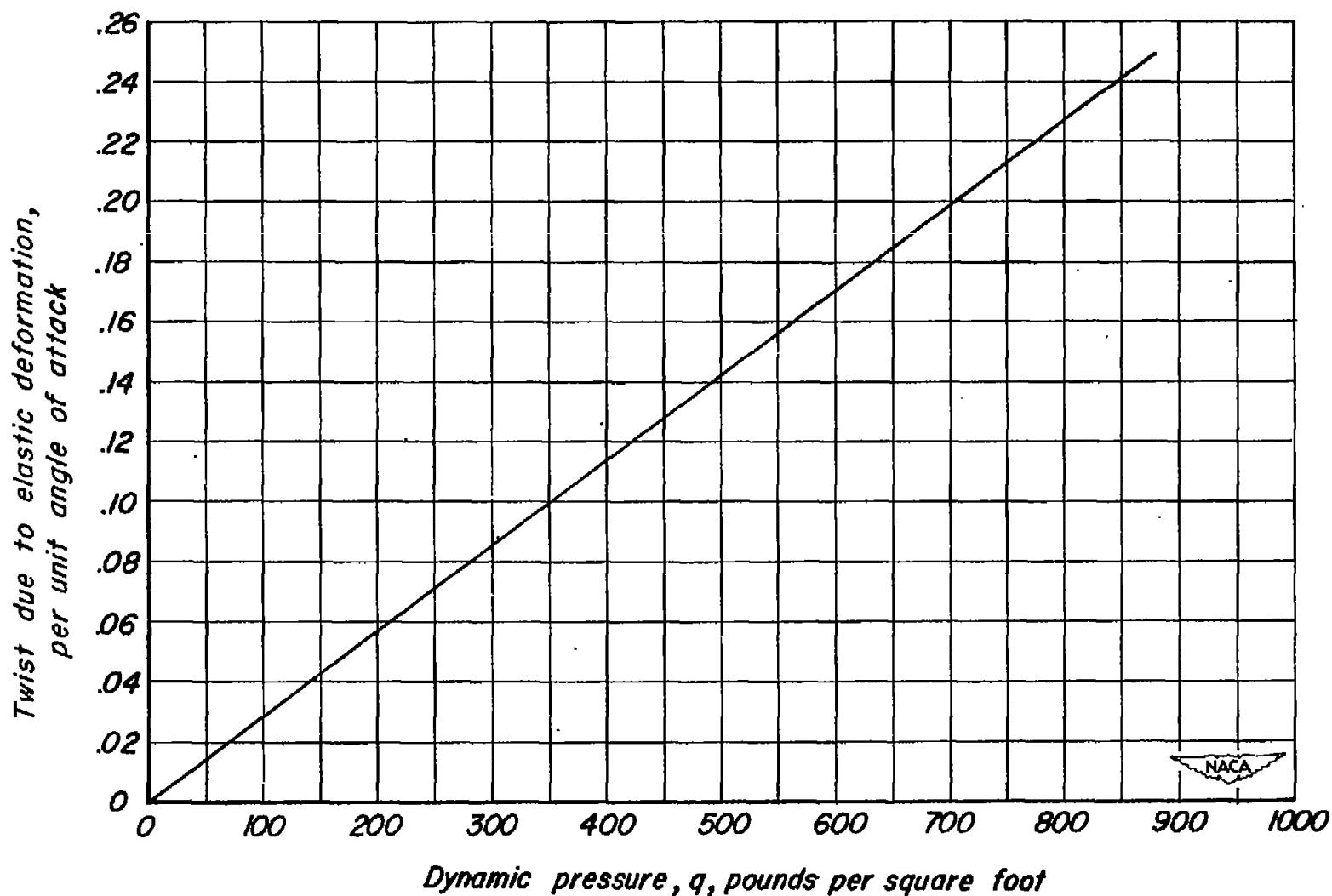
Figure I.—Variation of elastic twist with dynamic pressure of the twisted and cambered 63°
wing model.
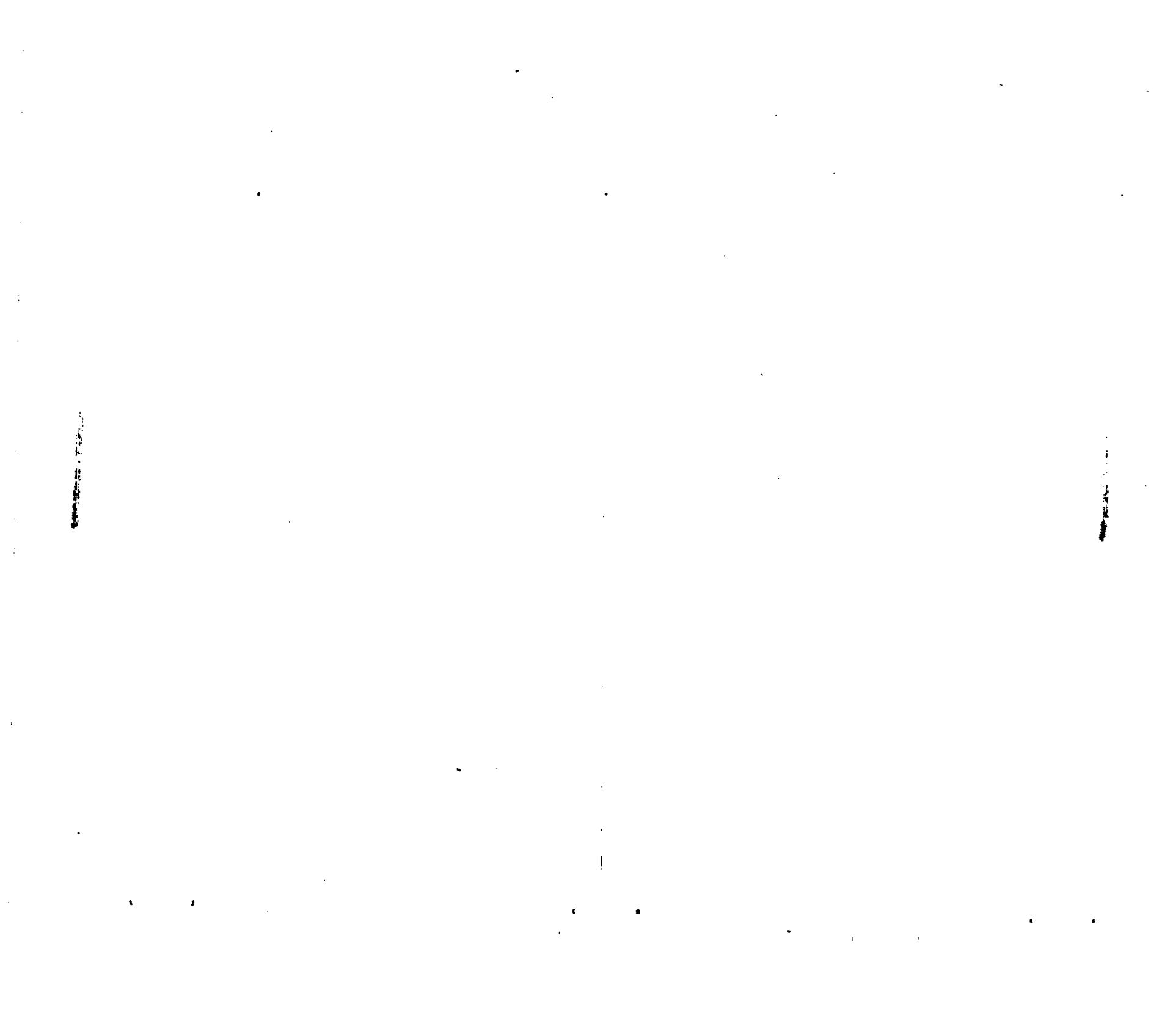
Figure 2.— The twisted and cambered 63° swept-wing model in the Ames 6— by 6-foot supersonic wind tunnel.

Fuselage

Equation $\frac{r}{r_o} = \left[1-\left(1-\frac{2x}{l}\right)^2\right]^{3/4}$

Fineness ratio: $\frac{l}{2r_o} = 12.5$

Wing

Thickness distribution NACA 64A005 (Streamwise)
Mean line a=1
Twist 3.52° (nonlinear)
Incidence 0°
Aspect ratio 3.5
Taper ratio 0.25

30.24"

$\bar{c} = 11.20"$

Moment center 33.04"

$r_o = 2.38"$

r

x

63°

16.50"

16.00"

35.00"

46.93"

$l = 59.50"$

4.00"
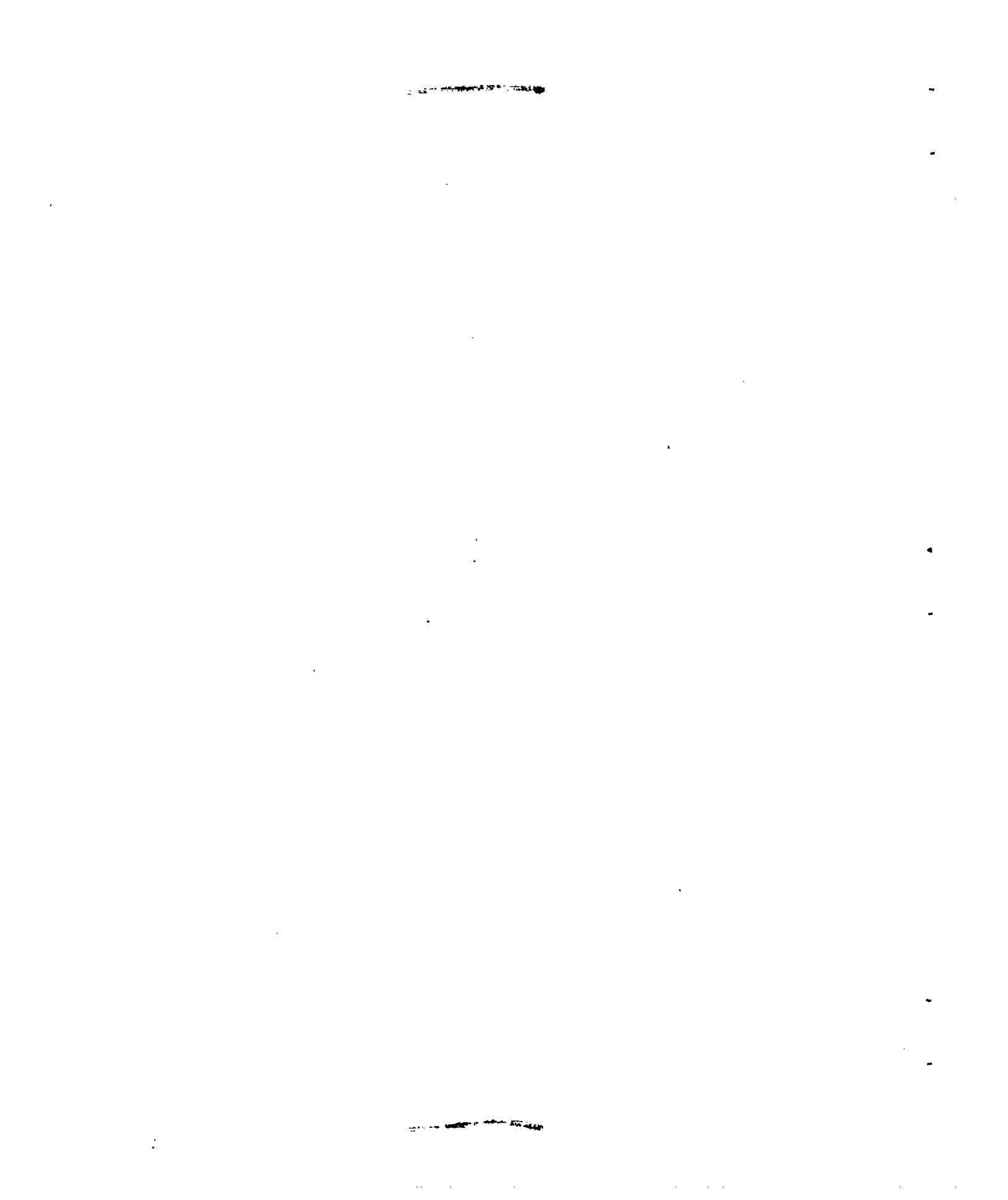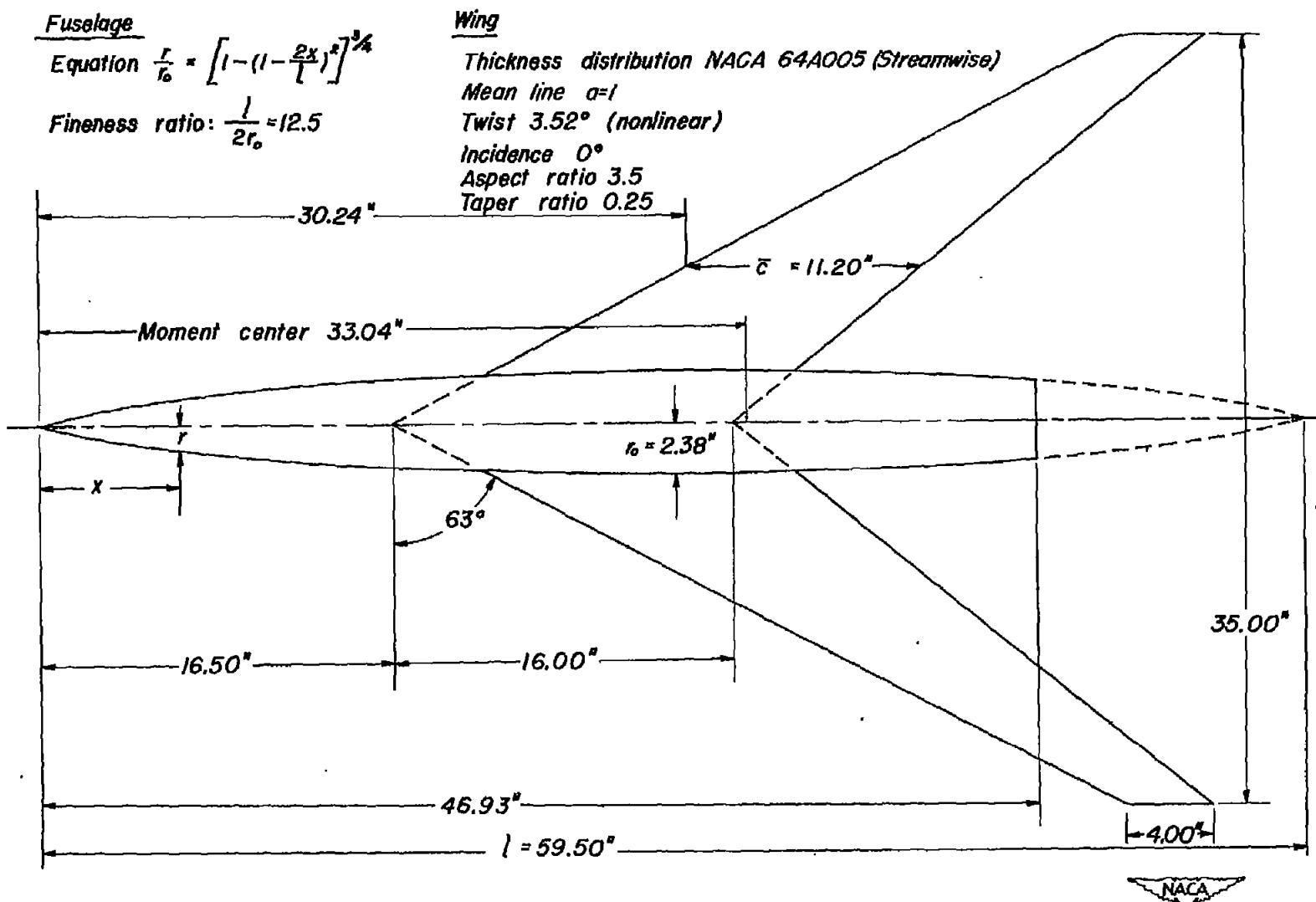
Figure 3.— Dimensions of the twisted and cambered 63° swept-back-wing model.
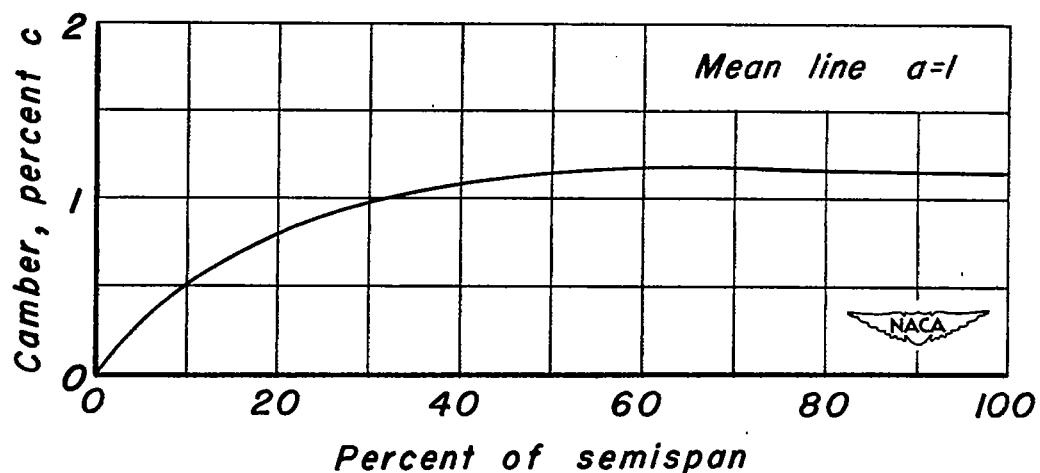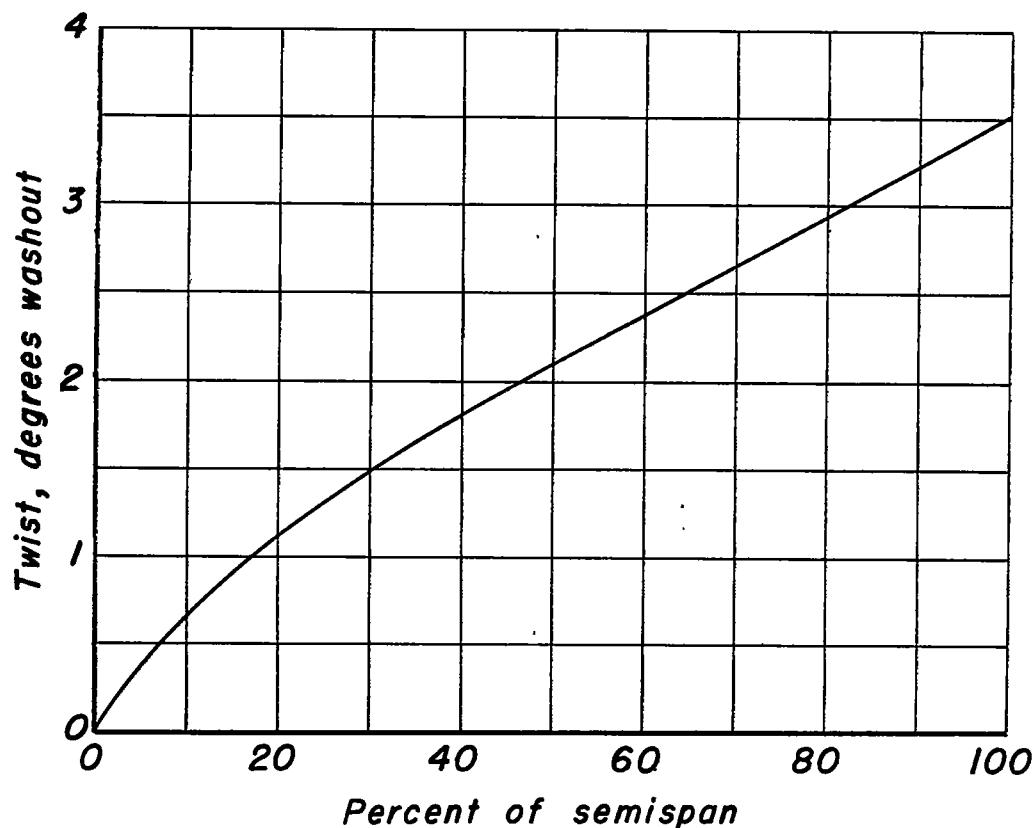
Figure 4.- The twist and camber distribution of streamwise
sections of the 63° swept-back wing.
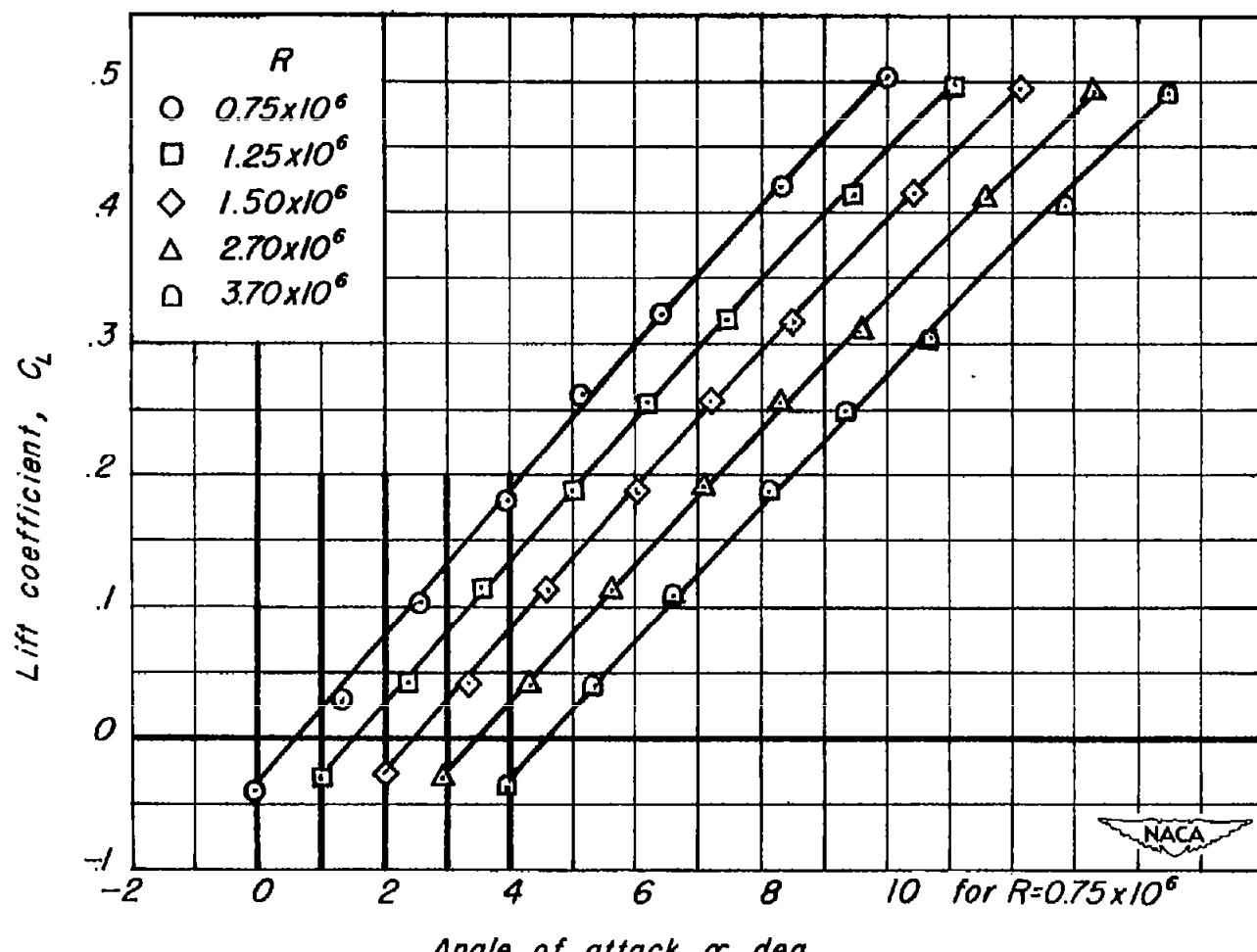
(a) M=1.20

Figure 5.-Variation of lift coefficient with angle of attack of the twisted and cambered 63° wing-fuselage model.
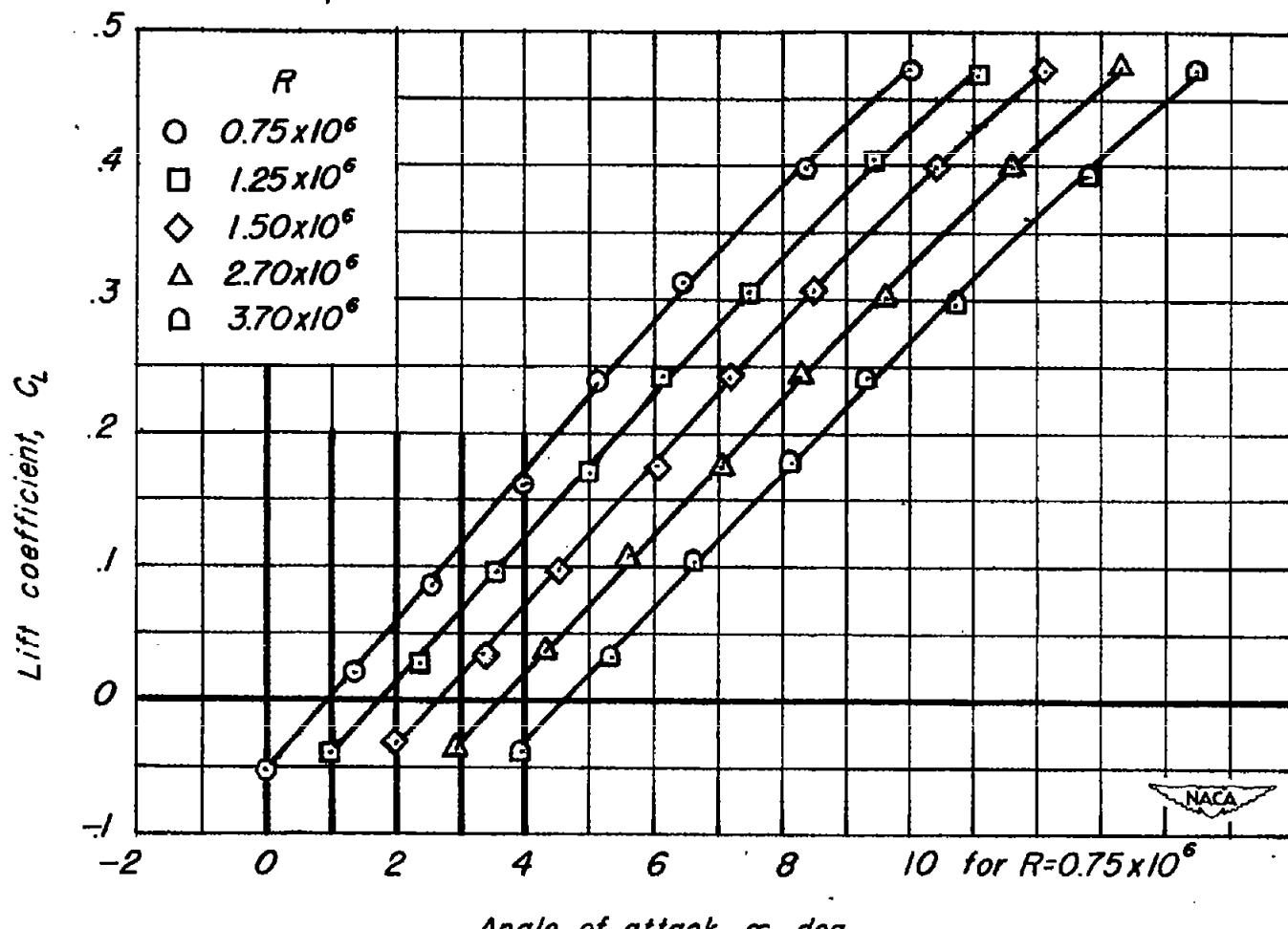
(b) M=1.30

Figure 5.—Continued.
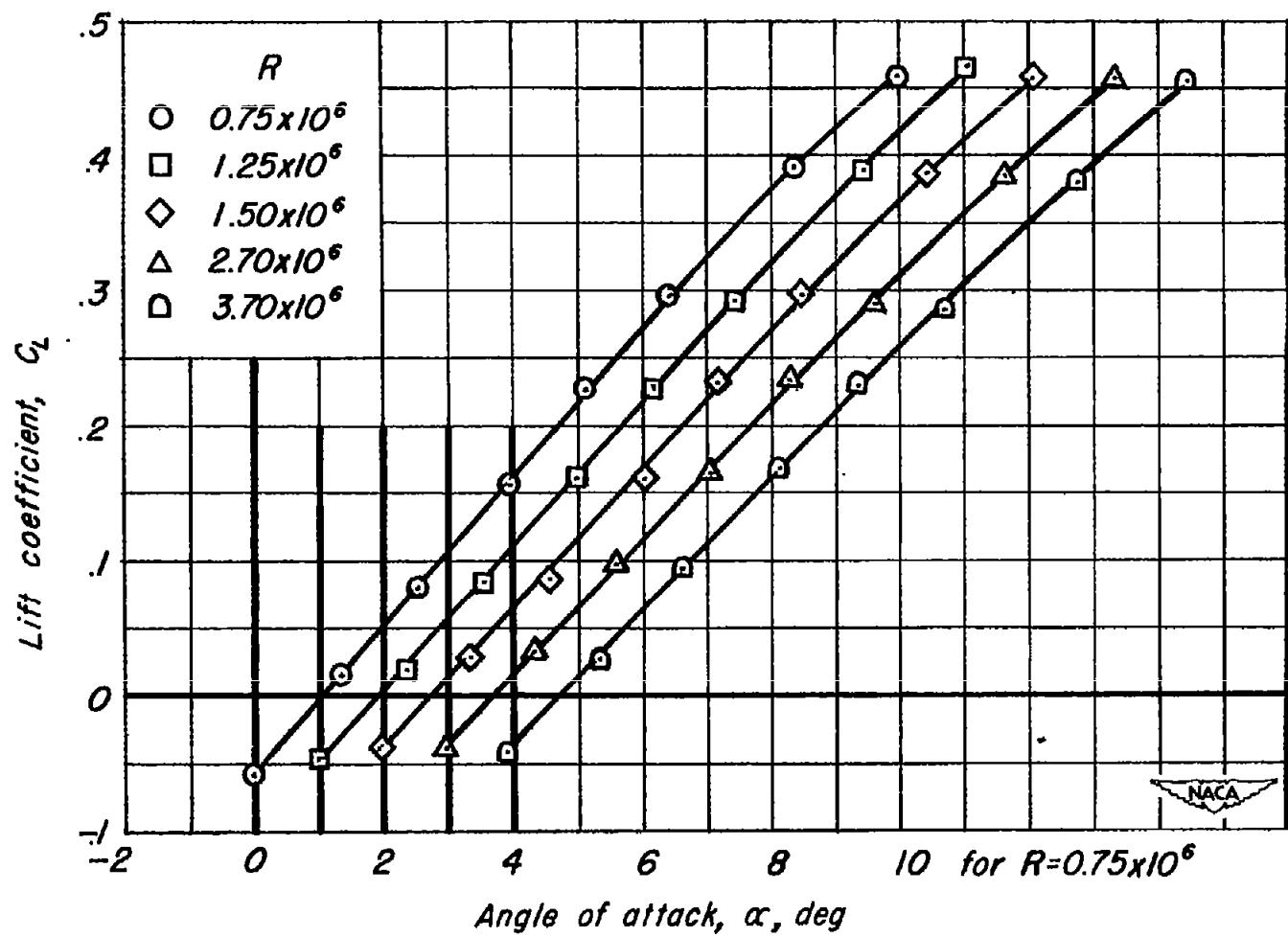
(c) M=1.40
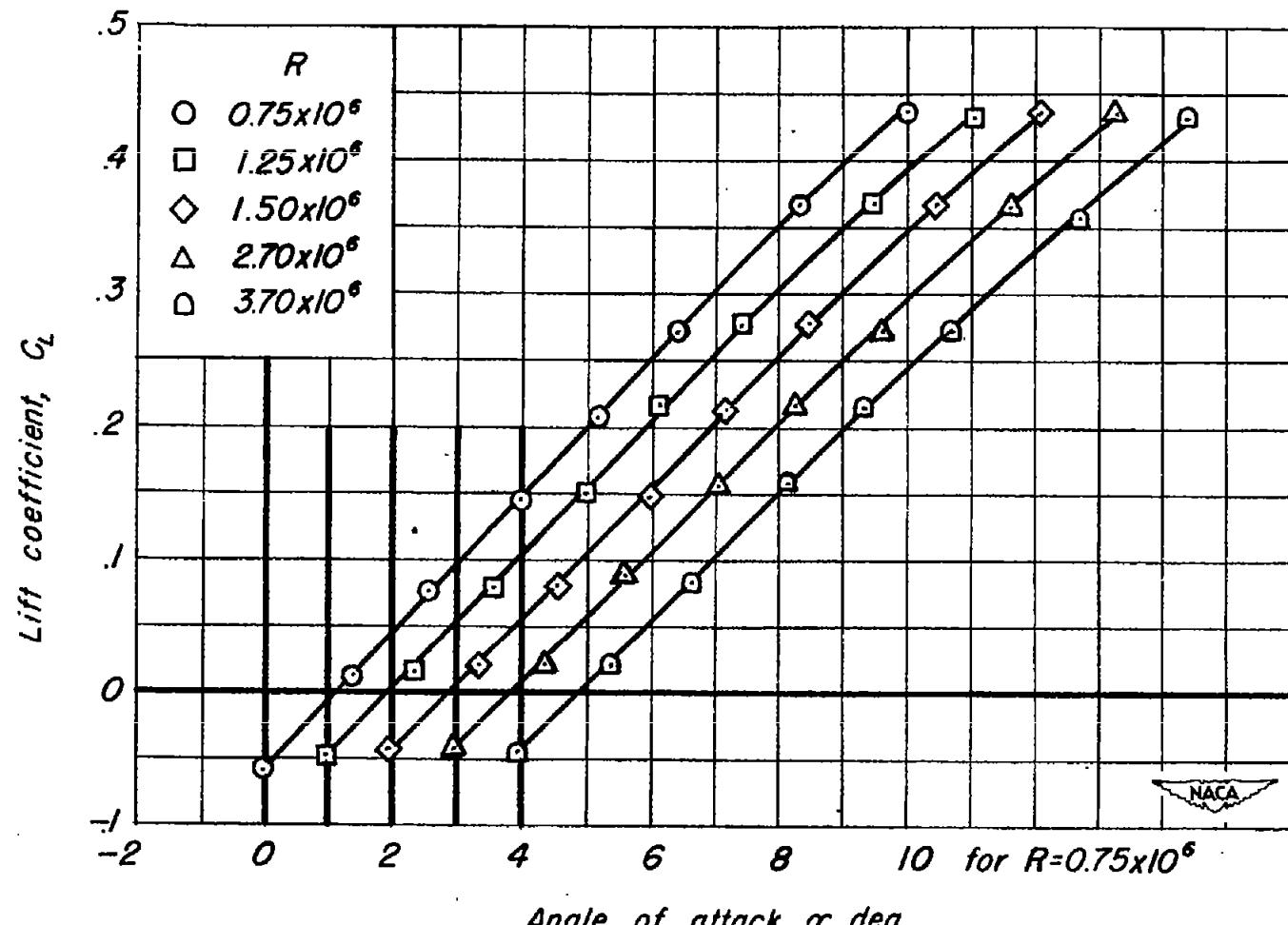
Figure 5.—Continued.

(d) M=1.53

Figure 5.— Concluded.
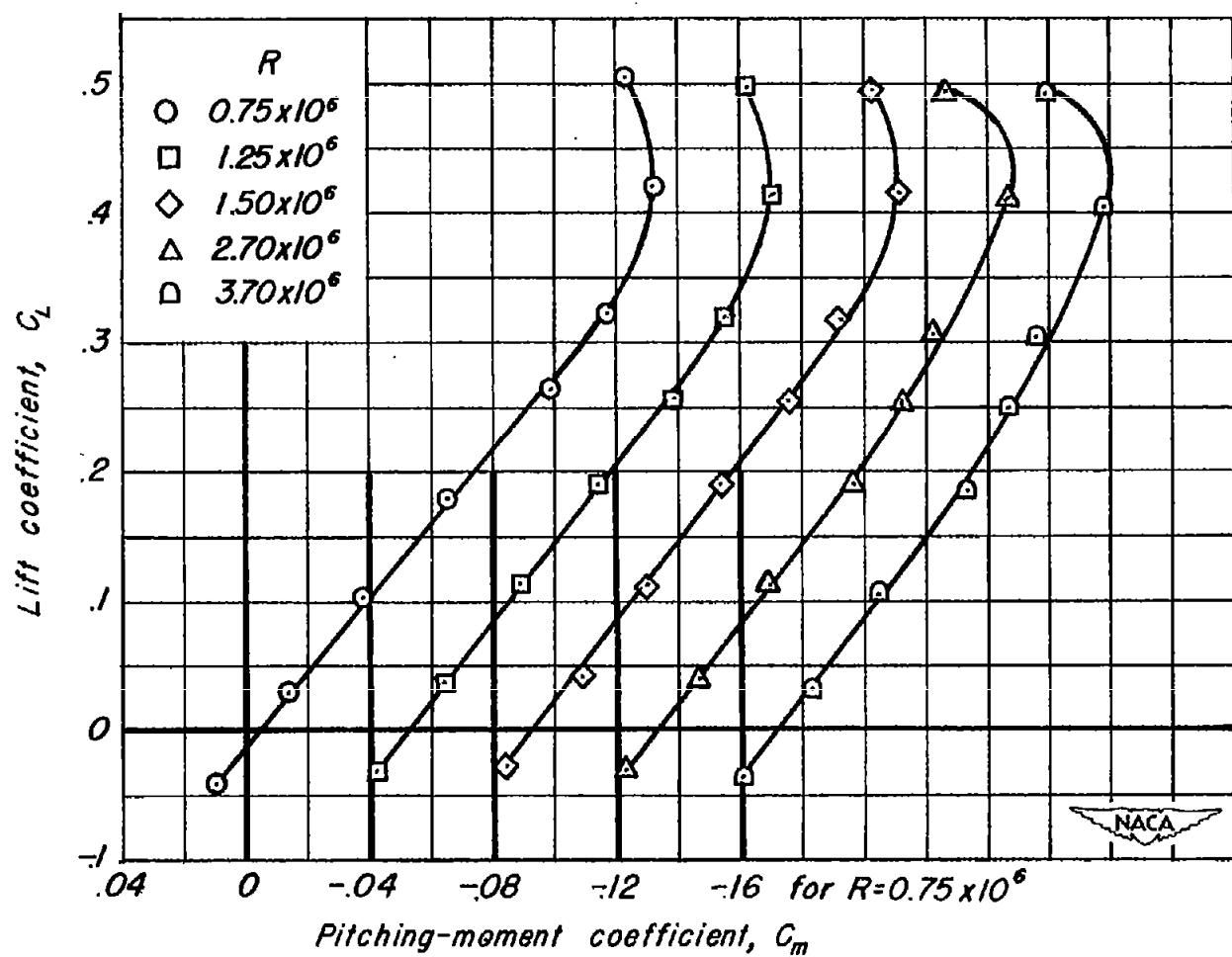
(a) M=1.20

Figure 6.-Variation of pitching-moment coefficient with lift coefficient of the twisted and cambered 63° wing-fuselage model.
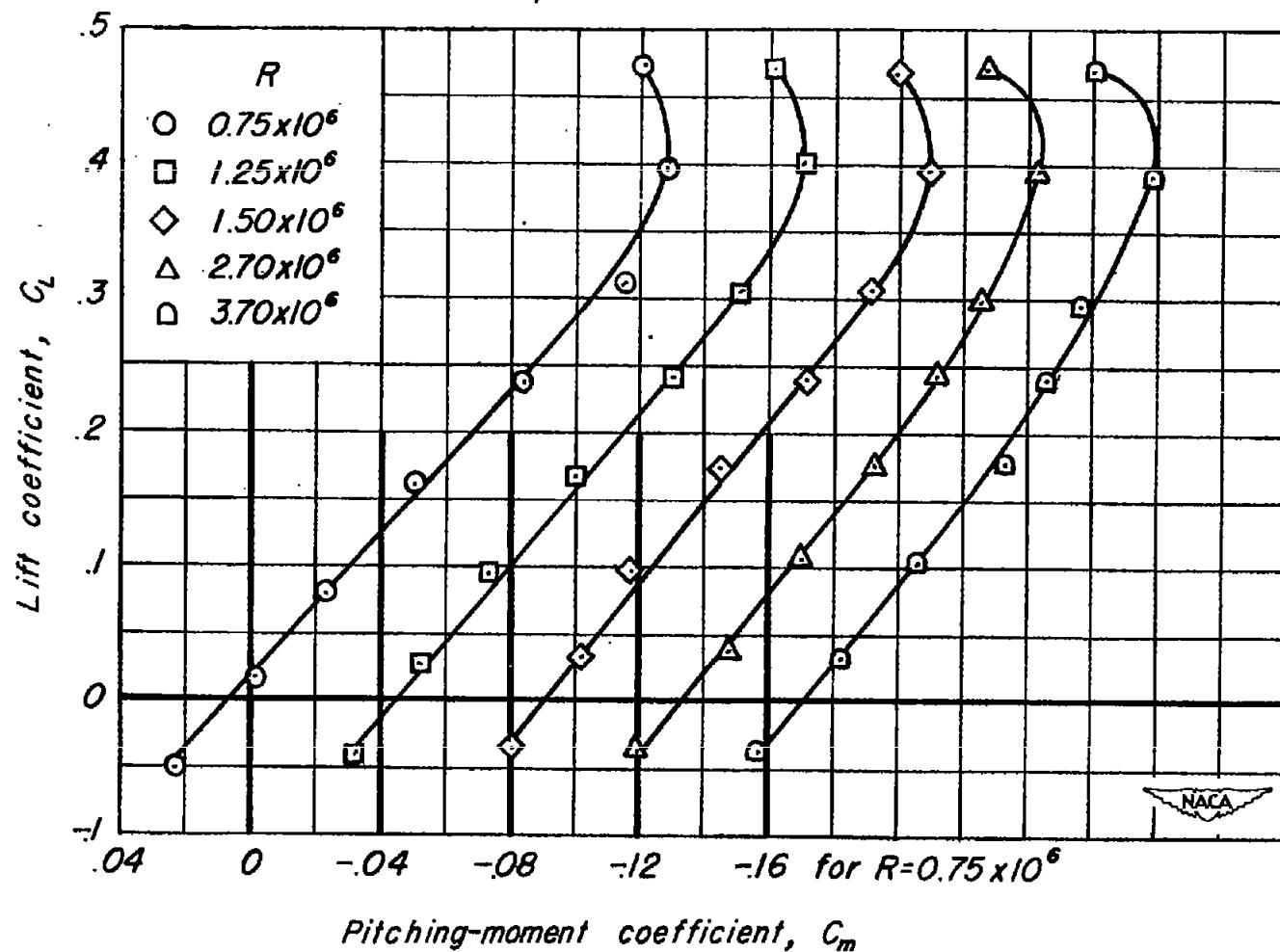
(b) M=1.30

Figure 6.— Continued.

(c) M=1.40

Figure 6.- Continued.

Figure 6. - Concluded.

(d) M=1.53
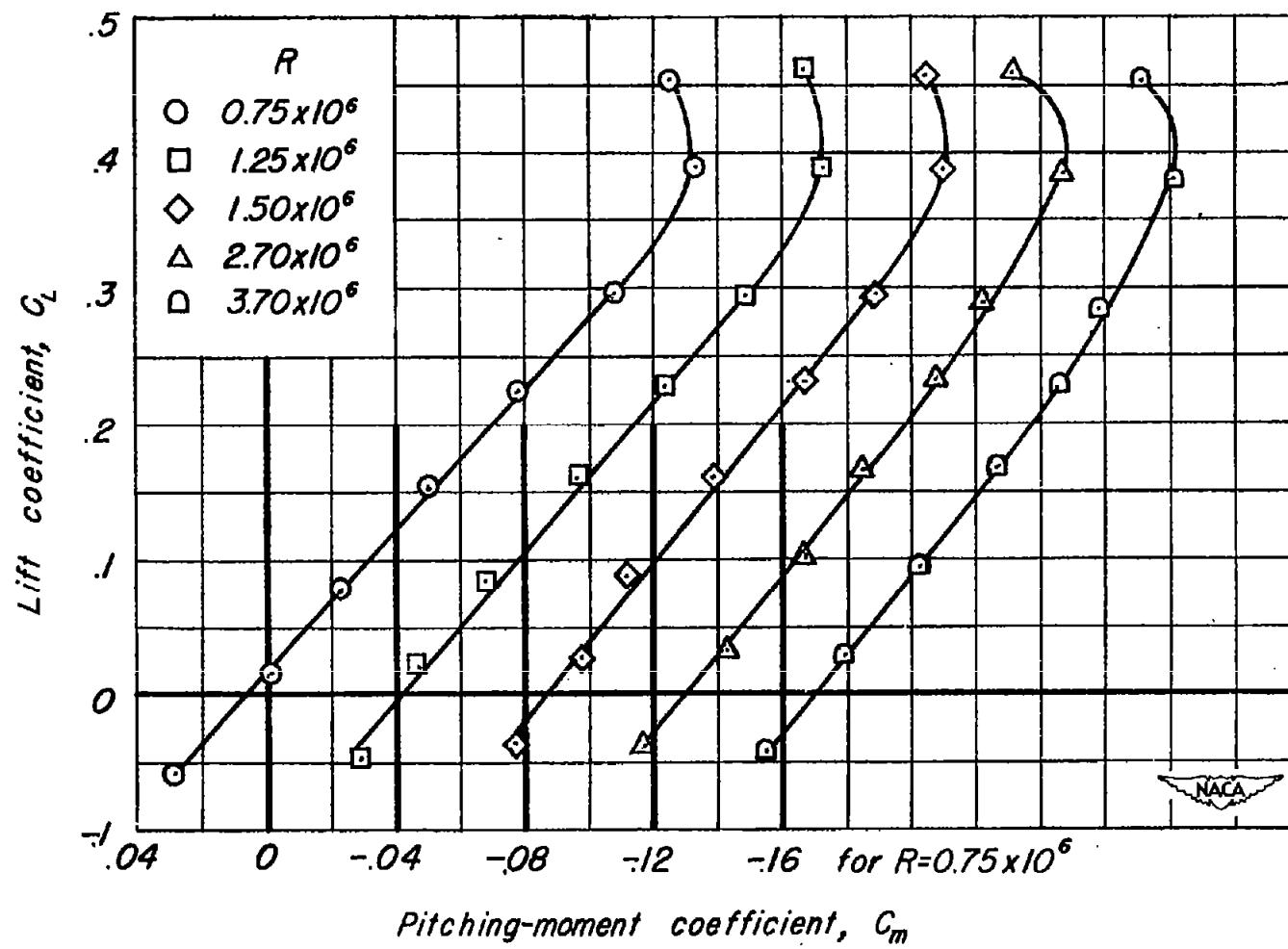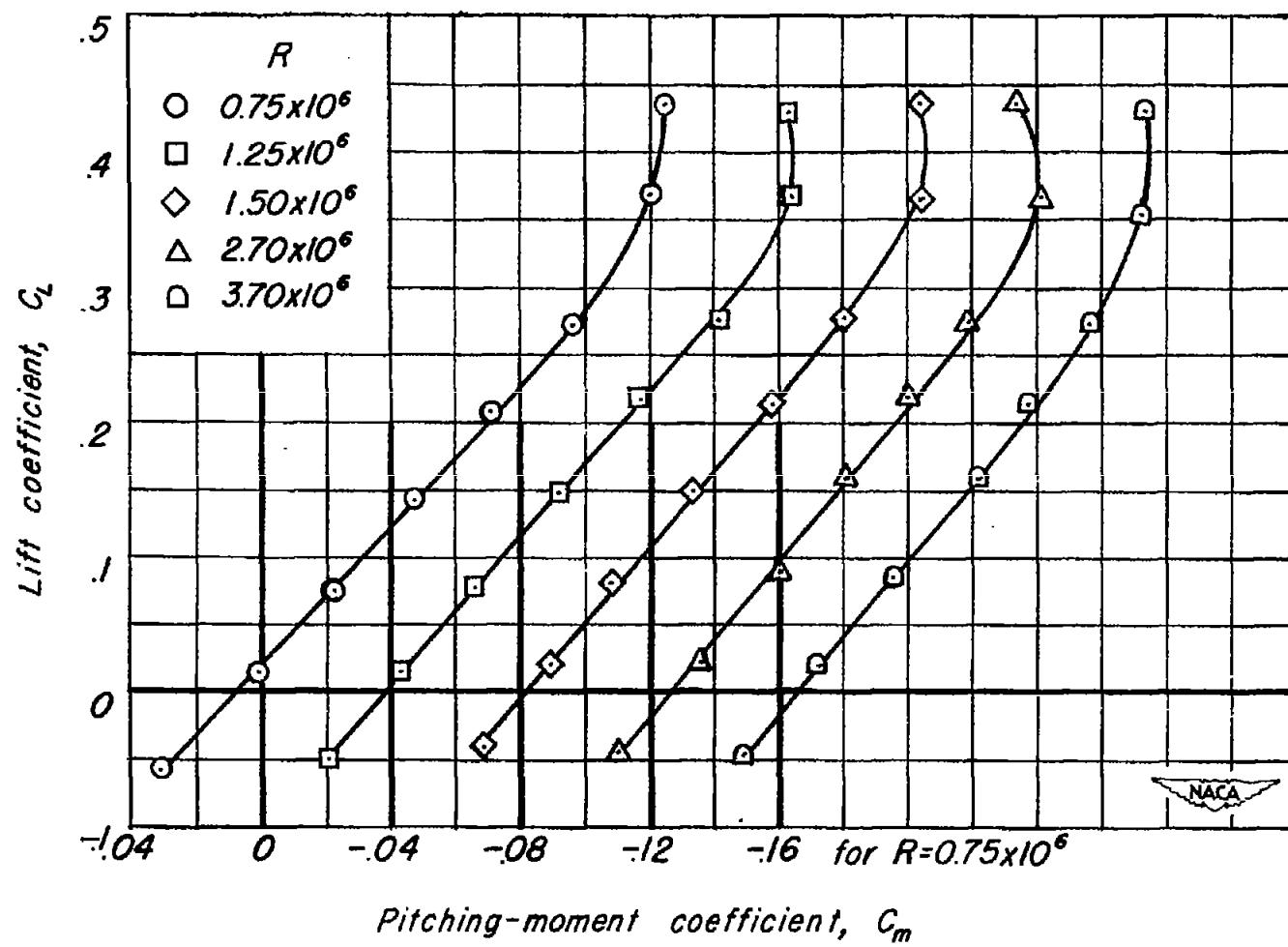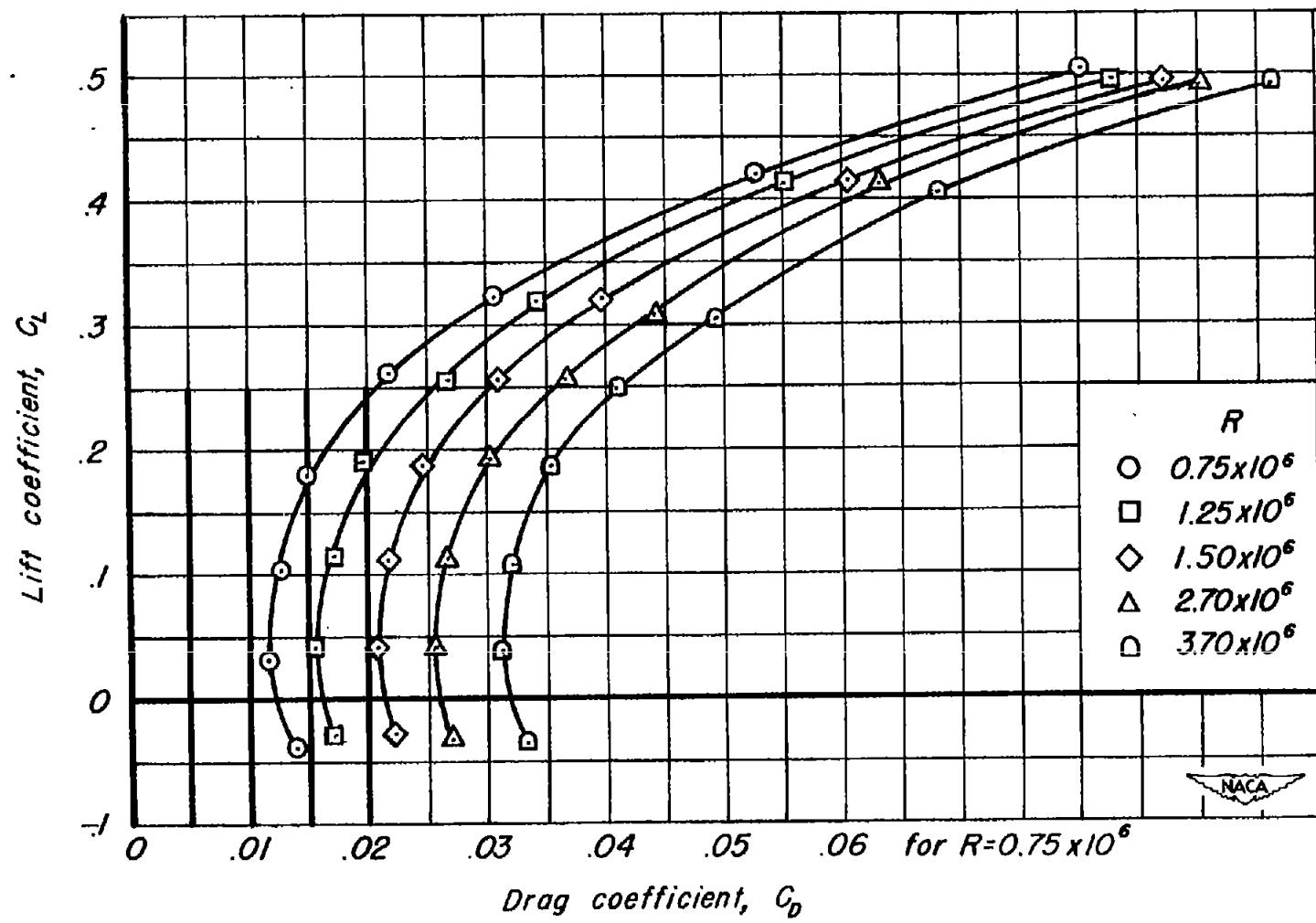
(a) M=1.20

Figure 7.—Variation of drag coefficient with lift coefficient of the twisted and cambered 63° wing-fuselage model.
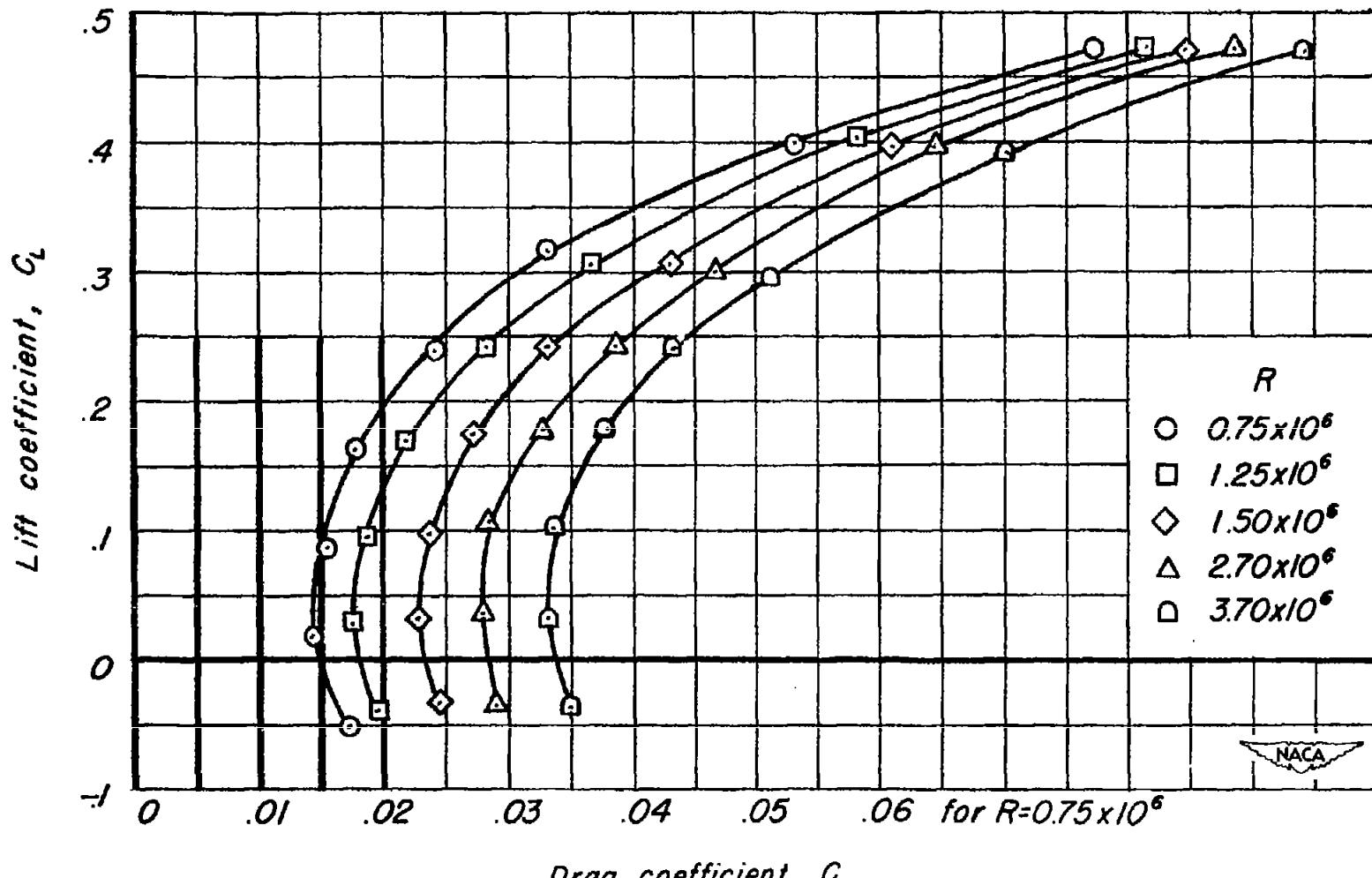
(b) M=1.30

Figure 7.- Continued.

(c) M=1.40

Figure 7. - Continued.

(d) M=1.53
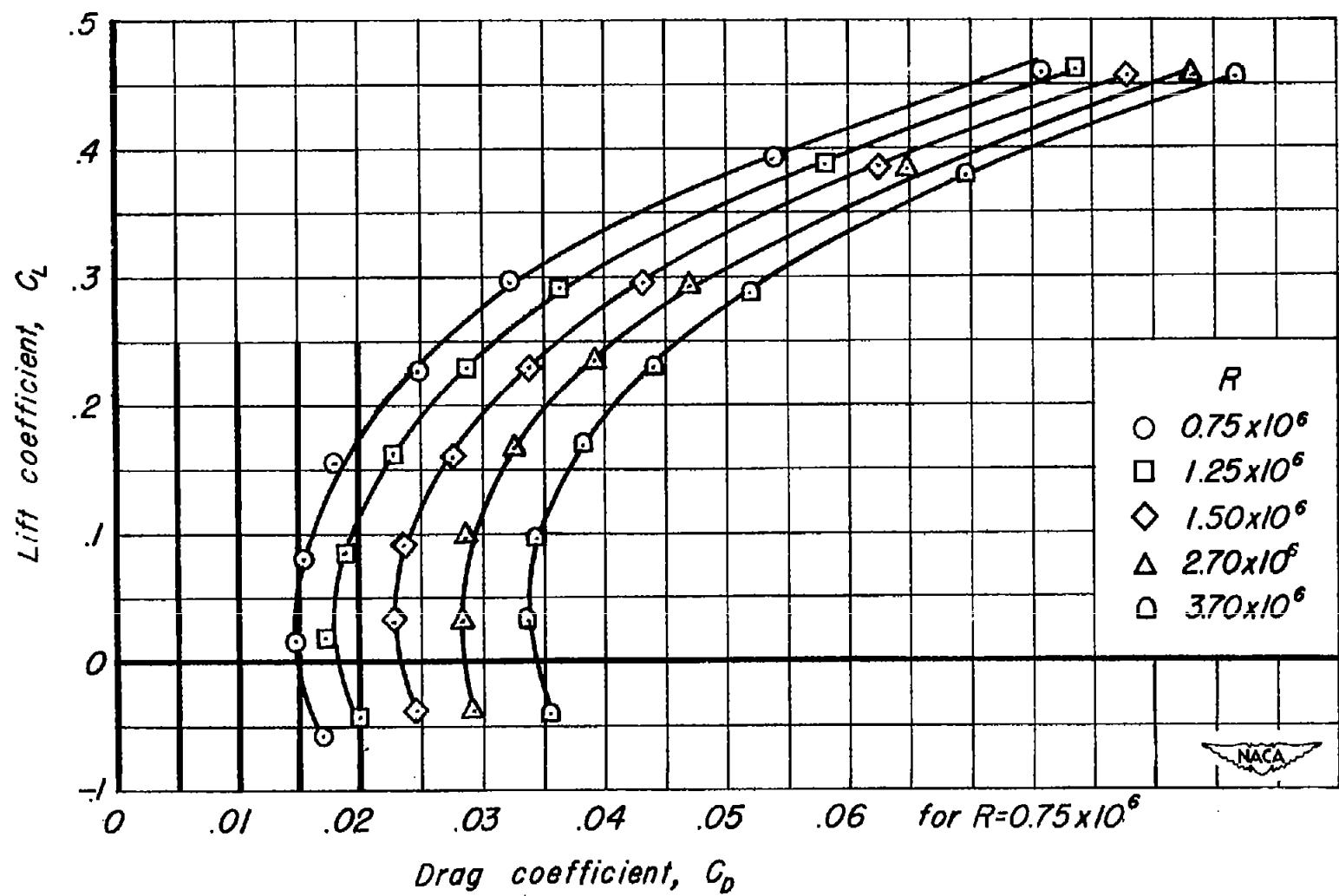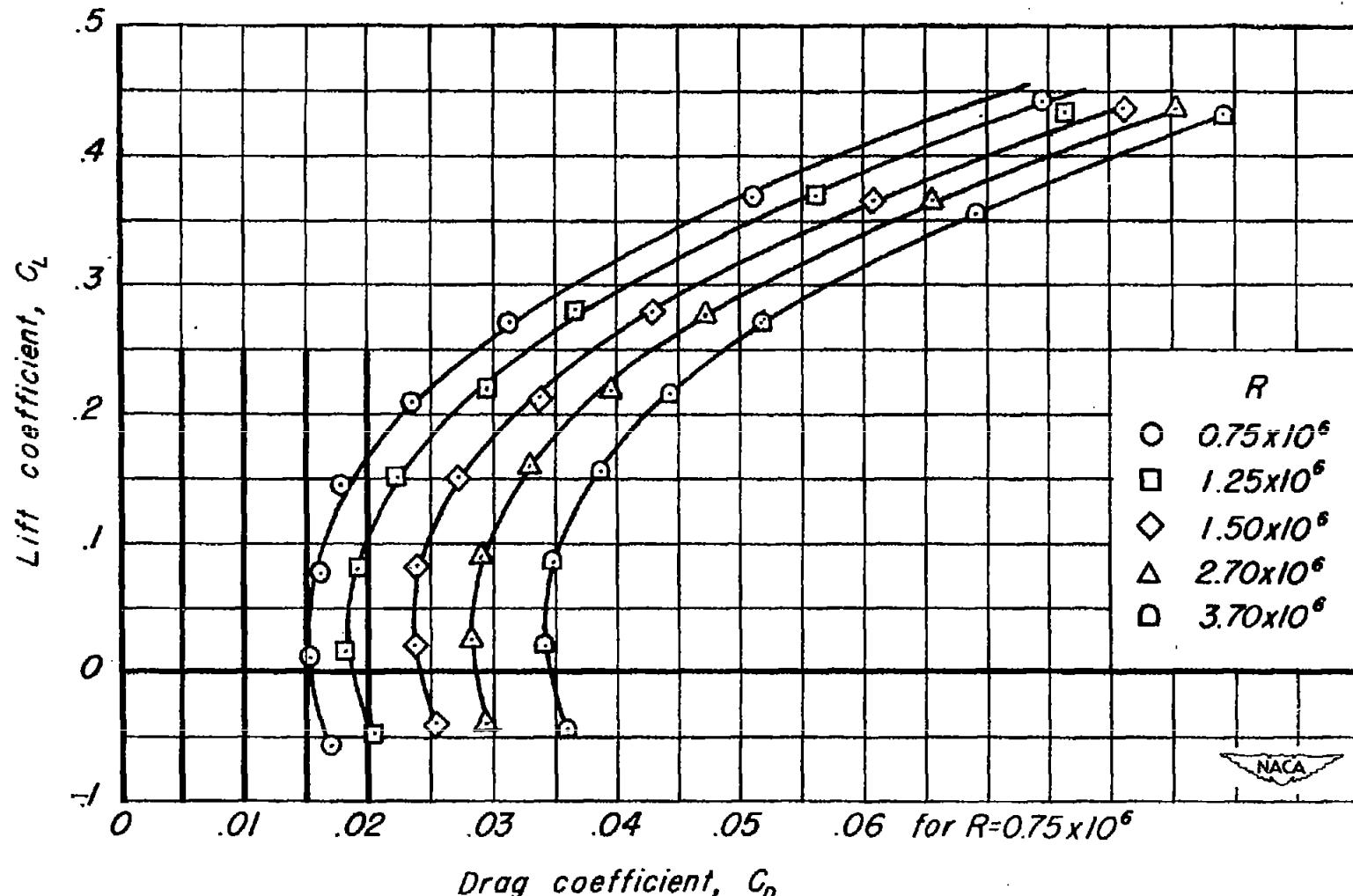
Figure 7.- Concluded.

(a) M=1.20
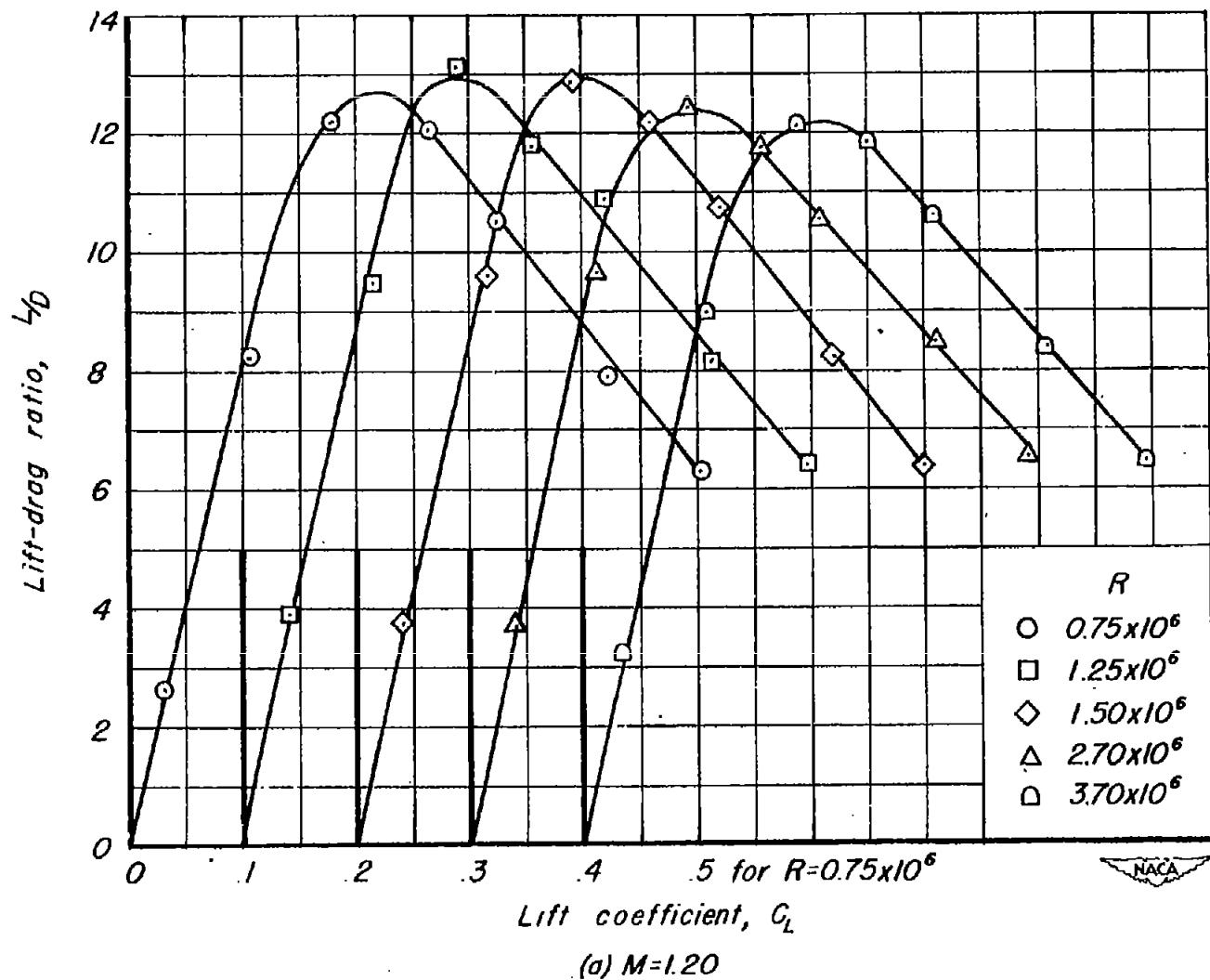
Figure 8.-Variation of lift-drag ratio with lift coefficient of the twisted and cambered 63° wing-fuselage model.

(b) M=1.30
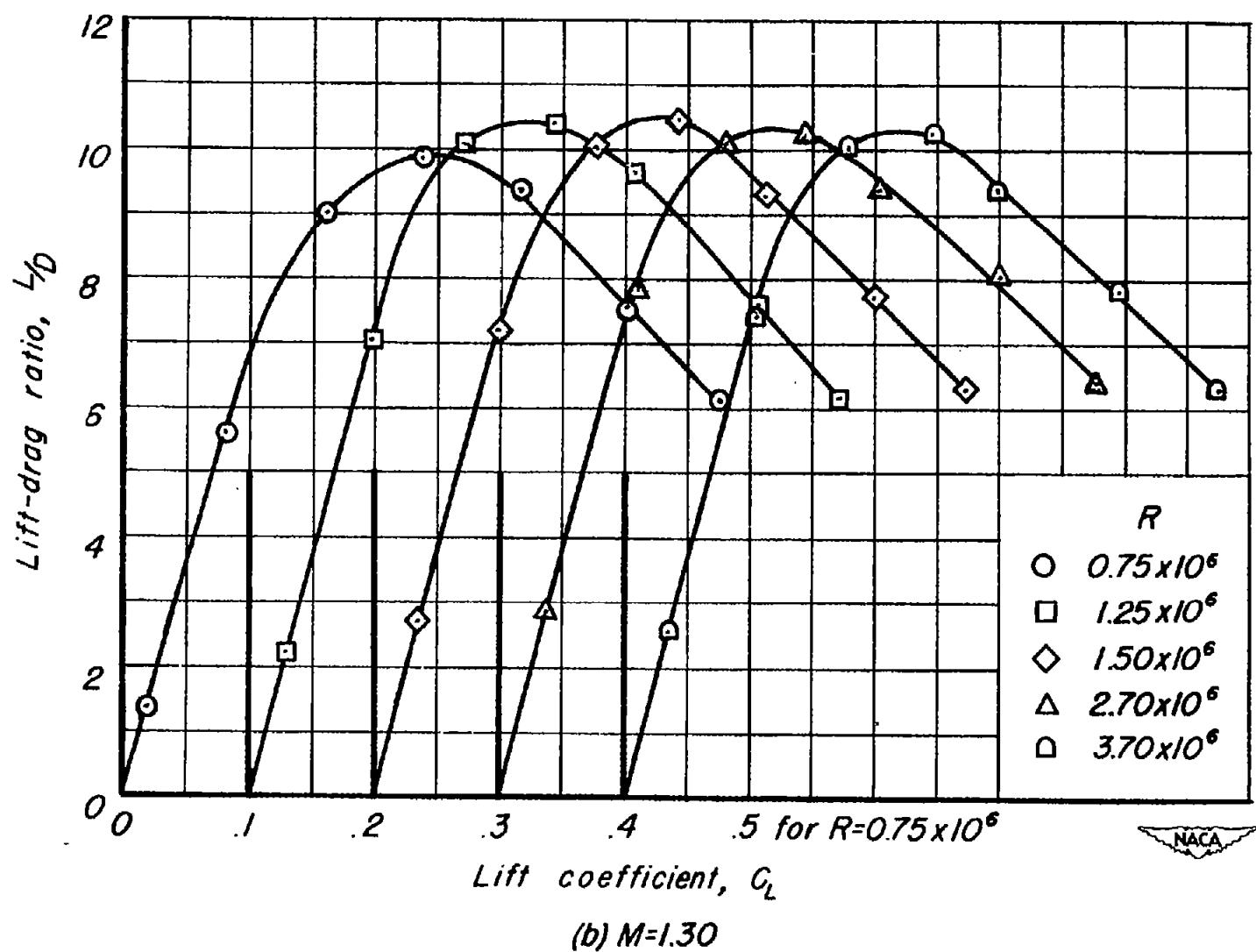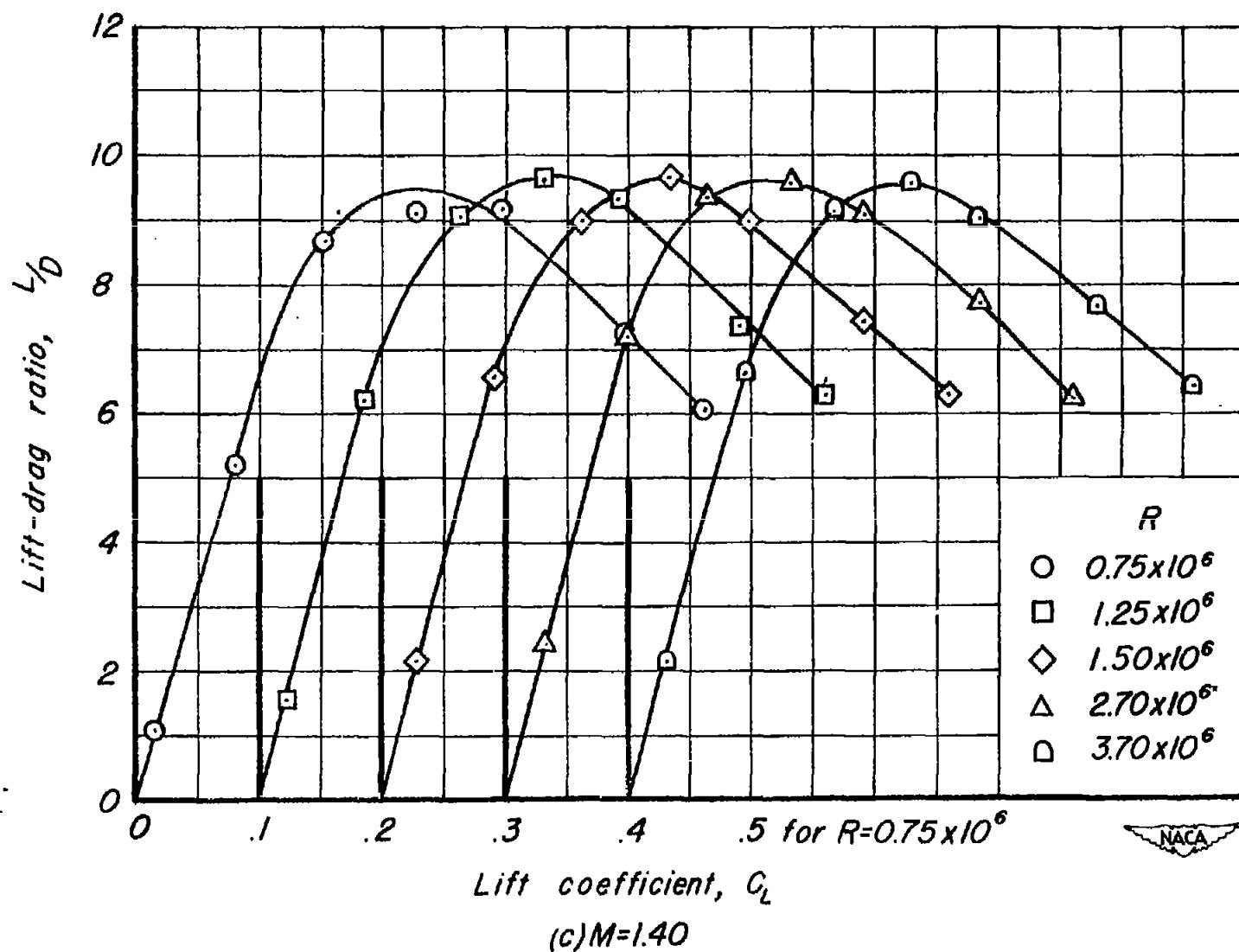
Figure 8.- Continued.

Figure 8.- Continued.

(c) M=1.40

(d) M=1.53
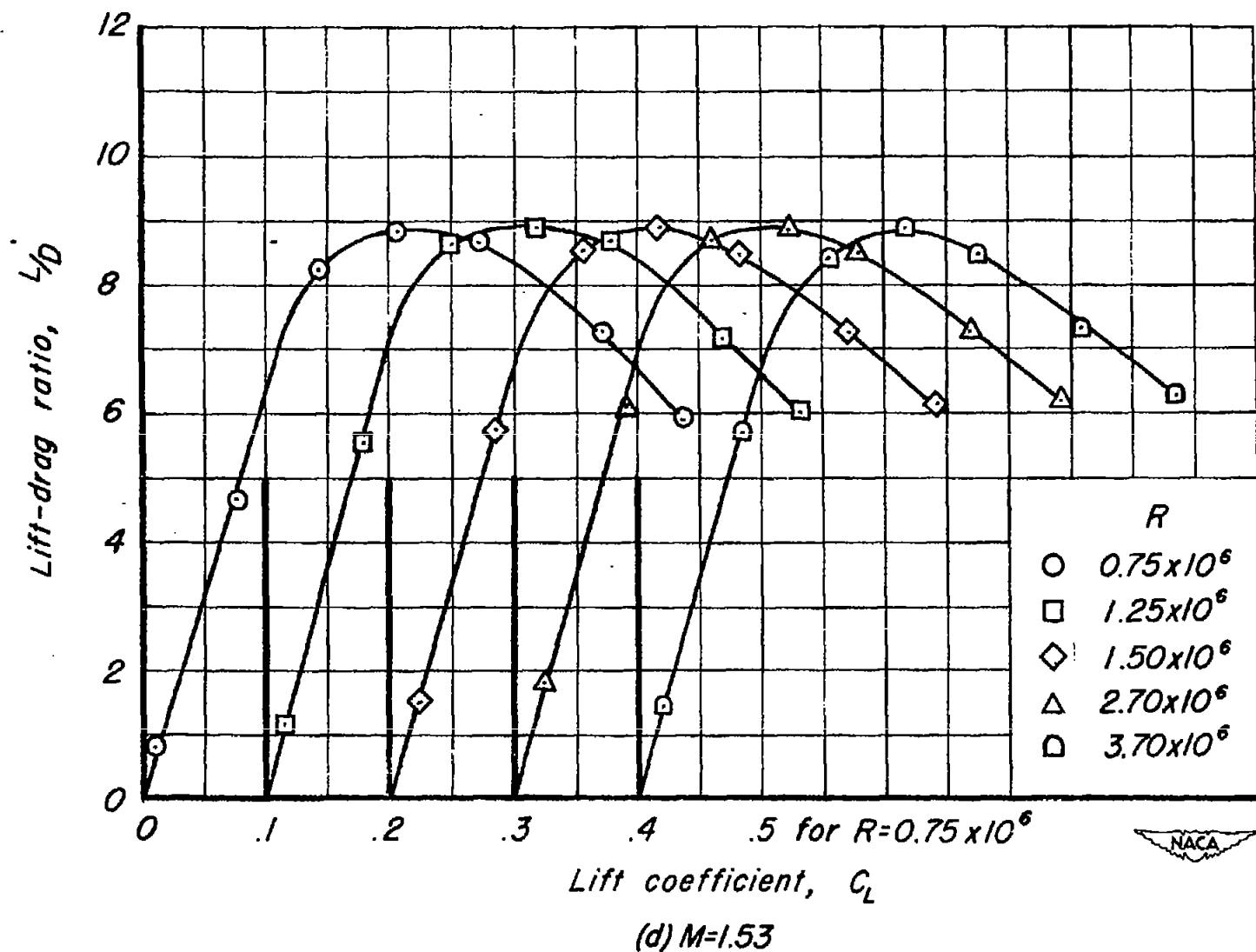
Figure 8.-Concluded.

5
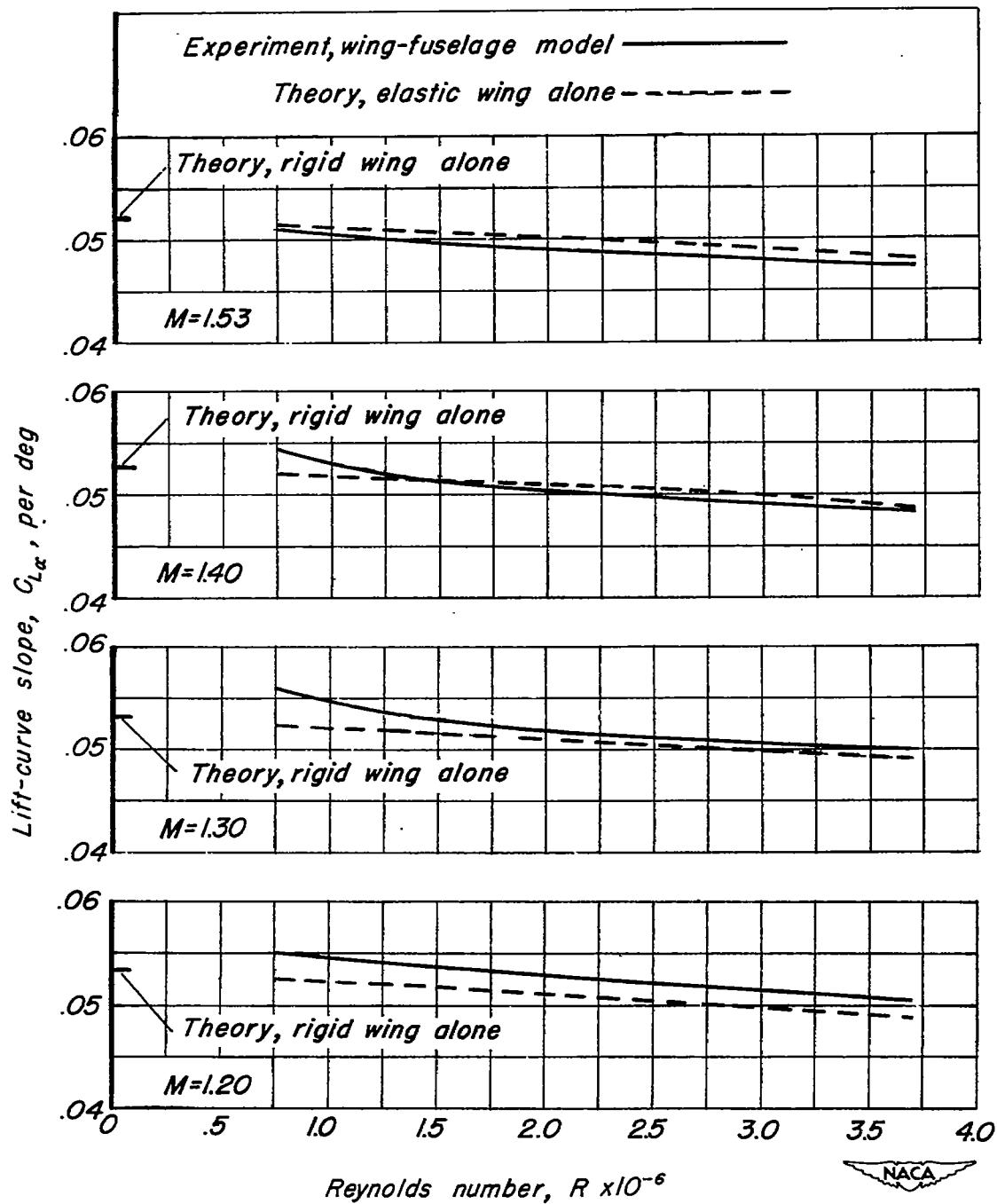
Figure 9.–Variation of theoretical and experimental lift-curve slope with Reynolds number of the twisted and cambered 63° wing-fuselage model.
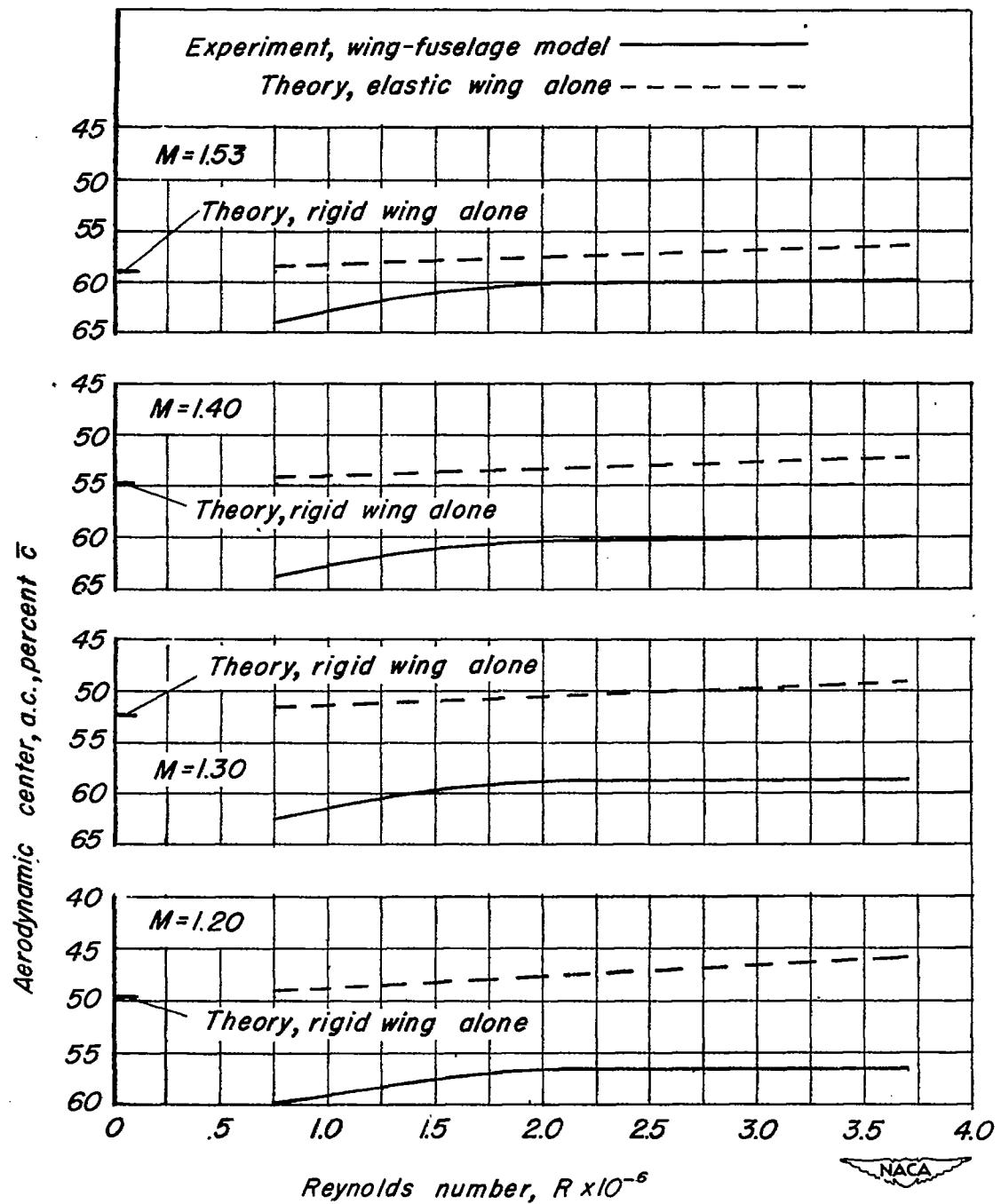
Figure 10.—Variation of theoretical and experimental position of the aerodynamic center with Reynolds number of the twisted and cambered 63° wing-fuselage model.
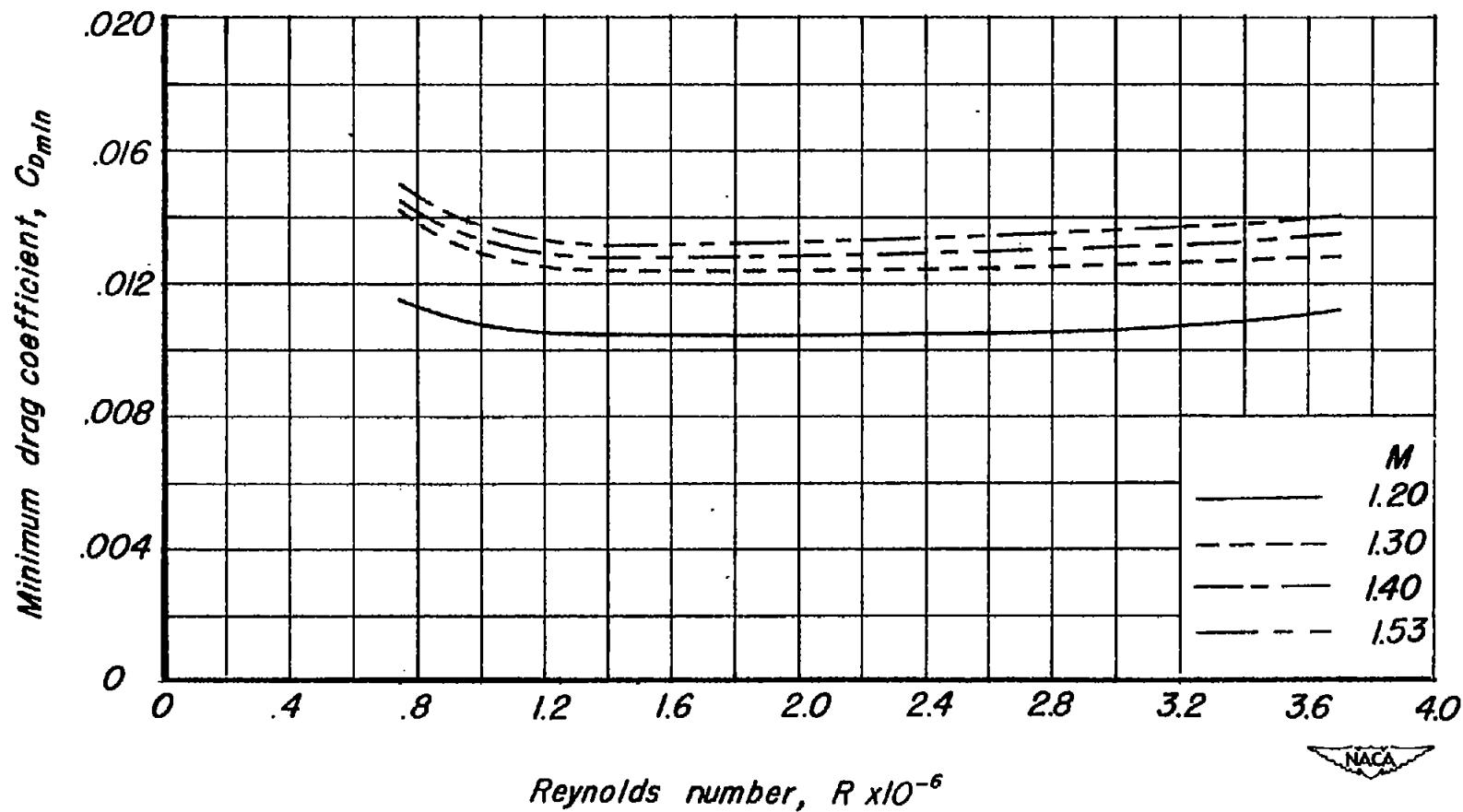
Figure II.—Variation of minimum drag coefficient with Reynolds number of the twisted and cambered 63° wing-fuselage model.
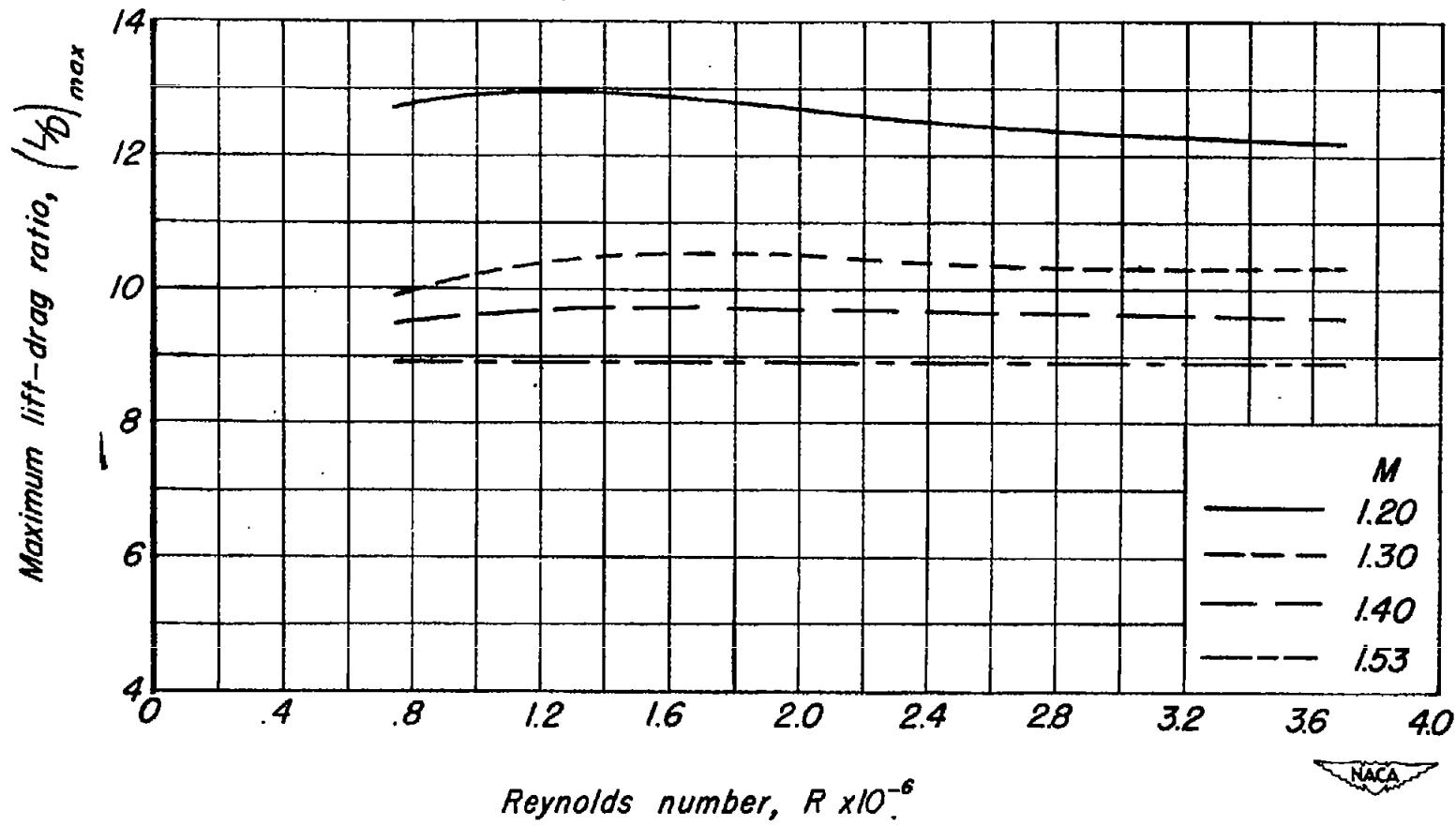
Figure 12.- Variation of maximum lift-drag ratio with Reynolds number of the twisted and cambered 63° wing-fuselage model.